MISCELLANEOUS PAPER NO. 4-893

BUMPS AND GRINDS: STUDIES IN BODY MOTION

by

W. G. Shockley

May 1967

Sponsored by

U. S. Army Materiel Command

and

Advanced Research Projects Agency

Conducted by

U. S. Army Engineer Waterways Experiment Station

CORPS OF ENGINEERS

Vicksburg, Mississippi

MISCELLANEOUS PAPER NO. 4-893

BUMPS AND GRINDS: STUDIES IN BODY MOTION

by

W. G. Shockley

May 1967

Sponsored by

U. S. Army Materiel Command

and

Advanced Research Projects Agency

Conducted by

U. S. Army Engineer Waterways Experiment Station

CORPS OF ENGINEERS

Vicksburg, Mississippi

ARMY-MRC VICKSBURG, MISS.

FOREWORD

This paper was presented by Mr. W. G. Shockley at the Fifth Meeting of the Quadripartite Standing Working Group on Ground Mobility, which was held in Kingston and Parry Sound, Ontario, Canada, during 9-19 August 1965. The information contained herein summarizes studies conducted for the U. S. Army Engineer Waterways Experiment Station (WES) by Chrysler Corporation under Contract No. DA-22-079-eng-403 and by FMC Corporation under Contract No. DA-22-079-eng-411.

The Chrysler study was a portion of the Mobility Environmental Research Study (MERS), sponsored by the Office, Secretary of Defense, Advanced Research Projects Agency, Directorate of Remote Area Conflict, under Order No. 400. WES is the prime contractor for the MERS project and the U. S. Army Materiel Command (AMC) is the service agent. The Chrysler study was reported in "A Study of the Vehicle Ride Dynamics Aspects of Ground Mobility," WES Contract Report No. 3-114, volumes 1 and 2 dated March 1965 and volumes 3 and 4 dated April 1965.

The FMC study was conducted in furtherance of Department of the Army Research and Development Projects 1-V-0-25001-A-131, Military Evaluation of Geographic Areas, which is sponsored by AMC. The study was reported in "A Computer Analysis of Vehicle Dynamics While Traversing Hard Surface Terrain Profiles," WES Contract Report No. 3-155, dated February 1966.

Colonel John R. Oswalt, Jr., CE, was Director of the WES at the time of the preparation and presentation of this paper. Mr. J. B. Tiffany was Technical Director.

BUMPS AND GRINDS: STUDIES IN BODY MOTION

by

W. G. Shockley*

Introduction

1. About four years ago, when the Waterways Experiment Station (WES) made its first tentative steps toward the development of a quantitative cross-country mobility prediction system for vehicles, a series of cross-country speed tests was conducted at the Yuma Test Station in the American desert. Among other things, these tests revealed that small-scale surface geometry features were among the most important, if not the most important, of the terrain attributes controlling the cross-country speed of military vehicles. It was found that the vehicles rarely attained the speed permitted by the strength of the surface they were crossing; instead, they were continually either accelerating away from a surface geometry feature or decelerating in preparation for encountering one. It was obvious from the tests that one of the most critical vehicle characteristics was "ride" quality; that is, the dynamic response of the machine to a vertical obstacle (i.e. a surface feature which results in vehicle motion in the vertical plane as the vehicle surmounts it).

2. As a result of this experience, the WES began an investigation of the state of the art with respect to ride dynamics, since it was quite obvious that any satisfactory mathematical model of terrain-vehicle relations would have to include the suspension characteristics of the vehicle. Our investigations revealed that the automotive industry and such laboratories as the Land Locomotion Laboratory had been working on the general problem for some time, and that they had made great strides in both the measurement and evaluation of ride quality. The approach taken by these organizations was that "ride" quality was a function of a spectrum of vibrations (i.e. small amplitude but relatively high frequency cyclic motion), and therefore the analytical approach was to treat both terrain input and dynamic vehicle response in terms of wave motion. The most useful device was to reduce both terrain characteristics and vehicle response to power spectral density (PSD) relations, and then correlate the two statements by involving a jury.

---

* Engineer, Chief, Mobility and Environmental Division, U. S. Army Engineer Waterways Experiment Station, Vicksburg, Miss.

3. When we examined this problem in the light of our experiences in cross-country mobility, a school of thought arose which questioned whether this approach could provide an adequate evaluation of cross-country vehicles. Experience seemed to indicate that speed was limited by the magnitudes of the bumps which were generated as the vehicles surmounted discrete vertical obstacles, rather than by the cumulative grind of vibration. One of the mathematicians working on related matters (Dr. James Dugundji, University of Southern California) insisted that no form of vibrational analysis would elucidate the cause-effect relations when a vehicle hits a bump. He found a substantial body of support at the WES, and as a result we are currently favored by at least three schools of thought on this question.

4. The first school is convinced that vibrational analysis is an adequate approach, because it is held that the response of a vehicle to a discrete vertical obstacle is simply a high-frequency, low-amplitude vibration, and is therefore susceptible of treatment by PSD analysis. The second school insists that design improvement in suspension systems is dependent upon the ability to follow the force systems through the individual vehicle components, and that therefore one needs a form of analysis based on fundamental force systems. That is, one must be able to predict what a unique surface feature will produce in the way of vehicle response. The third school straddles the fence; it argues that the PSD analysis is entirely adequate for small-amplitude surface irregularities, but that the discrete prediction scheme will have to be used for large obstacles.

5. The question between bumps and grinds could not be resolved by debate, so it was decided to investigate the potentiality of both. The internal capabilities at the WES were inadequate to the task, so the problem was turned over to two contractors: the FMC Corporation is investigating the "bump" approach; the Chrysler Corporation is extending its previous work on the "grind" approach.

Bumps: The FMC Corporation Study of Ride Dynamics

6. The point of departure for this study was the desire to develop a completely objective method of predicting the absolute displacements

generated at any position in a vehicle as a response to an encounter with any surface geometry feature at any speed. The implications of this are:

a. That an accurate mathematical model of the surface be employed as terrain input.

b. That the mathematical model of the vehicle be a component-by-component construction, so that information on displacement can be recovered at any point.

7. Any attempt to mathematically model a terrain for the purpose of predicting vehicle dynamic response raises two questions:

a. Can the model be made to fit the real terrain within acceptable limits of accuracy?

b. Will the analytically predicted response of the vehicle traversing this terrain agree within acceptable limits of accuracy to reality?

8. Because there existed no prior data on the degree of fit required by item a in paragraph 7, it was decided to model the surface geometry by fitting a Fourier series to it. The advantage is simply that the accuracy of fit is a function of the number of terms in the Fourier series; greater or lesser degrees of fit can be achieved by adding or subtracting terms from the Fourier expression. Therefore, a Fourier series was used having the general form:

$$X = \frac{a_o}{2} + \sum_{i=1}^{n} b_i \sin\left(\frac{2\pi i}{p} y + \alpha_i\right) \qquad (1)$$

where:

X = microgeometry evaluation at horizontal displacement y

a_o = twice the average value of X

b_i = sine coefficient for the i term

α_i = phase angle for the i term

i = series term number

p = fundamental period length

n = total number of terms in series

This sine-phase angle form was preferred over the sine-cosine form because computer time was saved in evaluating the trigonometric functions. A pure sine or cosine series could not be used since both odd and even functions were components of the overall curve fit. This property was introduced because a method for extending the profile had to be employed; the Fourier series describes a cyclic function extending from + ∞ to - ∞, while the surface geometry profile is of finite length. The method chosen was to repeat the given profile indefinitely, so that:

$$f(y + np) = f(y) \tag{2}$$

as illustrated in fig. 1.

9. It was also necessary to make the start and end of the profile at the same level, $f(np) = f(0)$, so that an abrupt change would not occur at the end of one cycle and the start of another. This level was selected at zero, $f(np) = 0$, so that the initial conditions of a vehicle traversing the terrain could all be set equal to zero.

10. The digital computer program for evaluating the Fourier series terms to fit this microrelief is presented in Appendix A. This program was designed to accept surface geometry profile data as they come in from the field. It had been found that the surveying method which was most conservative of time and effort was to locate, in terms of distance and elevation, each "break" in slope. On curved surfaces, many such points would be selected; on planar surfaces, the points would be far apart. Thus, the surveying results consist essentially of a series of irregularly spaced x-y coordinates. The existing program accepts these sets of coordinates locating the points of discontinuity and calculates linear functions between them. These linear functions are used as the $f(y)$ for the Fourier integrations. Up to 100 coordinate sets may be specified. The program output consists of the constant a_o, the sine coefficients b_i, and the phase angles a_i where i is the series term number. The total number of terms may be any number desired up to 52. Calculated amplitudes are compared with the input coordinates and the error of fit is included in the output.

11. As a test of the program, a simple surface geometry feature (fig. 2) was used to check the program. A 40-term Fourier series fit the bump profile with a maximum error of 1.5% (i.e. the maximum departure of the computed profile from the real profile was 1.5% of the total height of the real obstacle). In addition, a number of surface geometry configurations extracted from Appendix E of WES Technical Report 5-625 * were fitted with a 52-term Fourier series. The maximum fit error for each microgeometry feature was:

		Percent	Illustrated on fig. No.
Site 15_2:	Rice-field bund, A	1.68	3
	Rice-field bund, B	1.46	
	Field prepared for unidentified row crop	2.66	4
	Field surface fallow after ride	6.64	
Site 19_3:	Rice-field bund	2.45	
Site 21_5:	Canalized water channel	8.19	5
Site 45_1:	Stream channel	6.02	6
Site 53_2:	Boulder-strewn slope, A	4.57	
	Boulder-strewn slope, B	2.07	7
Site 92_4:	Terraced rice field, A	2.25	
	Terraced rice field, B	4.70	

These profiles were plotted by scaling the plates in TR 5-625. The terrain heights listed under "input" are the scaled values; the "output" heights are the corresponding values of the Fourier-series curve. A comparison of these two height columns indicate the absolute fit achieved. The accuracy of fit was considered satisfactory for all profiles.

12. The next step in the process was to develop a three-dimensional mathematical model of a vehicle (an M37 3/4-ton truck was used as an example) and test it using the Fourier expression as the surface geometry

* U. S. Army Engineer Waterways Experiment Station, CE, Environmental Factors Affecting Ground Mobility in Thailand, Technical Report No. 5-625 with Appendices A-H (Vicksburg, Mississippi, May 1963)

input. The truck body was allowed three degrees of freedom (bounce, pitch, and roll) and was supported by four spring-damper combinations representing the suspension. The suspension was supported by a differential assembly front and rear, each having two degrees of freedom (bounce and roll). The differential assemblies were supported by spring-damper combinations representing the tires. This model with the necessary symbols is shown in fig. 8. Equations for input parameters (tire deflections and deflection rates, and suspension deflections and deflection rates) are given in table 1. The model requires seven simultaneous second-order ordinary differential equations with first derivatives. These equations are given in table 2.

13. A preliminary computer program was developed to solve the seven differential equations of motion. This initial program placed no restraint on suspension deflection and assumed that the tires remain in contact with the ground. These conditions are probably realistic for slow travel and small responses. A Fourier series description of the surface geometry is used for the displacement forcing function with the option of different time lags for each wheel to simulate the traversing of the terrain at an angle to the ridge lines, thereby inducing a roll motion in the response. The program output consists of the displacement, velocity, and acceleration of the truck body in bounce, pitch, and roll. Figs. 9 through 14 illustrate the predictions of bounce and pitch displacements, velocities, and accelerations. The response curves derived from the standard two-dimensional, single-mass mathematical model which had previously been used are included for comparison.

14. The next logical step consists of two parts:

a. Refine the three-dimensional model to take care of such things as wheels leaving the ground, the suspension system "bottoming out," and the nonlinear deflections and recoveries of suspension system elements; and

b. Test the model against real performance values obtained in the field.

15. Both of these phases have been completed. The model is now about as elegant as it is practical to make it at the present time; it

already needs a computer of rather phenomenal capacity. A diagrammatic mathematical model of a generalized wheeled vehicle (only very slight modifications are required to accommodate tracks) is illustrated in fig. 15. Furthermore, the model was altered to include such things as:

a. Variable rolling radii, as illustrated in fig. 16

b. Horizontal and vertical force reactions at the wheel ground contact points (fig. 16)

c. Wheel bounce, so that it loses contact with the surface (fig. 17)

d. Nonlinear and/or discontinuous suspension spring constants, to take into account the situations in which the vehicle "bottoms out" (fig. 17)

e. Nonlinear and discontinuous responses of shock absorbers (fig. 18)

f. Variable horizontal speed.

The new equations describing body bounce, body pitch, and body roll are presented in table 3. This new model was then "run" over two of the terrain types previously used for evaluating the simplified model (figs. 4 and 7) and the predicted motions (i.e. roll, pitch, bounce, and horizontal speed) recorded.

16. Next, models of these terrain features were constructed of reinforced concrete, in two different versions. The first was so arranged that the obstacles were encountered at right angles to the axis of motion (fig. 19), and the second version was so arranged that the angle of impact was 60° (fig. 20).

17. The test vehicle, an M37, 3/4-ton 4x4 truck, was disassembled and all of the required parameters were measured in the laboratory, to make certain that the vehicle descriptors were correct. The vehicle was then put back together, appropriately instrumented, and run through the courses under extremely carefully controlled conditions, with the motions being recorded continuously by two different recording schemes. One employed vehicle-mounted accelerometers; the other used continuous high-speed photography.

18. The results are still being analyzed, but it is obvious even at the present time that the predicted responses and measured responses fit with remarkable fidelity. The maximum error is about 8%, well within the 10% error which had been accepted as tolerable. Fig. 21 illustrates a portion of one of the response curves.

19. If it be accepted that the mathematical model truly predicts dynamic vehicle responses within an acceptable level of accuracy, then it is clear that a powerful tool for assisting in the design of cross-country vehicles is in hand. It is anticipated, for example, that a designer will be able to vary response characteristics or other vehicle parameters one at a time, and evaluate the results on the machine as a whole. It seems obvious that design solutions very close to optimum could be achieved relatively quickly and cheaply by this method.

Grinds: The Chrysler Corporation Investigations of Ride Dynamics

Introduction

20. Up to this point the WES activities concerned with the effects of singular vertical obstacles which cause a transient response of the vehicle system have been described. In this case, vehicle speed is primarily limited by the operator's anticipation of the "bump" which will result when his vehicle strikes the obstacle.

21. In addition to these studies, WES has conducted as part of the Mobility Environmental Research Study (MERS) being conducted for Advanced Research Projects Agency (ARPA) a study which is intended to elucidate the relations between terrain roughness and vehicle vibration. This study has been accomplished under contract by Defense Engineering, Chrysler Corporation, with Mr. B. D. Van Deusen as the principal investigator. The criterion for vehicle evaluation is that of human response to vehicle vibration; hence the "grinds." In this case, it is assumed that the vehicle operator will vary speed until the vibration of the vehicle (i.e. the "ride") is tolerable or acceptable. Factors which may determine sustainable speed include the ability of the operator to control the vehicle, human tolerance to vibration, and damage to or destruction of the vehicle or cargo.

22. The purpose of the Chrysler Corporation vehicle ride dynamics study was to assess the adequacy of present analytical systems for predicting the ride performance of military vehicles operating cross-country over irregular surface profiles at speeds up to 25 mph, and to establish areas that need further development to effect good correlation between the analytical prediction and actual vehicle behavior. The study was basically a state-of-the-art determination of analytical systems applicable to the problem of vehicle ride dynamics. As stated earlier, the study was not concerned with shock or impact aspects of vehicle dynamics caused by singular vertical obstacles but with the more or less steady-state vehicle vibration, the subjective quality of which is termed "ride" in the literature. A limited amount of effort was expended in field experimentation to develop new or improve existing analytical systems from state-of-the-art knowledge.

23. A review of pertinent literature indicated that some qualitative criteria have been developed which will allow approximate measurements of vehicle ride. However, it was recognized that a definite need exists for quantitative analytical procedures which would permit designers to predict ride performance of a vehicle over a given irregular surface, as a function of vehicle speed. A minimum of three elements of the problem must be attacked in order to obtain numerical descriptors as ride indices for vehicle comparison. First, it is necessary to quantify the subjective reactions of humans in order to obtain a meaningful scale describing ride quality. Second, mathematical models of terrain-vehicle interaction must be developed, so that the vibration response within the vehicle can be associated with a particular terrain input. Third, a practical method of obtaining and analyzing terrain profiles must be developed. When these elements of the problem have been resolved, it will be possible to make design decisions from computer model studies, since it will be possible to evaluate the effect of tradeoffs between ride and other vehicle design considerations such as cost, weight, complexity, and reliability.

Human response to vehicle vibration

24. One criterion of interest for vehicle evaluation is that of human response to vibration. Thus, criteria for defining human response are necessary in order to determine the nature of the output of terrain-vehicle models. It is obvious that the form of the output will to some extent determine the form of the model which is used. This, in turn, will determine to some extent the form of the terrain measurements used as inputs to the model.

25. A number of previous research programs have attempted to define human response to vibration. In most of these programs, ride simulators with sinusoidal inputs have been used and attempts made to correlate comfort with frequency. While this information does not directly pertain to the type of vibration associated with most cross-country vehicles, a good deal of background can be obtained from study of the literature describing these experiments. Three problems exist in the interpretation of experiments with ride simulators using sinusoidal inputs in the light of the present objective:

a. The determination of the relationship (if any) between sinusoidal inputs and random vibration, such as that excited by terrain irregularities. It is suspected that a sine wave of a single frequency is more objectionable to the human than a random input having the same vibratory energy.

b. Most shake table experiments have involved vibration in a single plane. It is strongly suspected that vibration imposed simultaneously in more than one mode will not be equivalent to the sum of responses to each mode individually.

c. The criteria used for determining equacomfort levels in most shake table experiments are vague and subjective. The usual descriptive terms are mildly annoying, alarming, unpleasant, intolerable, etc. It is difficult to interpret vehicle vibrational activity in terms of these subjective criteria, since different people respond in substantially different ways. It is suggested that a numerical scale of some form is necessary to determine meaningful differences between vibrational levels.

26. Fig. 22 shows a composite of eight different ride simulator results for vibration tolerance. There are three conclusions that can be drawn from this graph:

a. There is a large discrepancy in discomfort level, which is attributed to the vague subjective criteria used. Interpretation of these results has been confounded by the large variety of experimental conditions used by the various investigators.

b. A plot of acceleration versus frequency at a given comfort level is relatively flat. It seems probable that the derivative of interest is the acceleration and not the displacement, velocity, or jerk (time rate change of acceleration).

c. There is an area between 5 and 7 cps where the human is more sensitive to vibration. This sensitivity is attributed to visceral resonance or resonance of the abdominal cavity. Vibration in this frequency range is quite disturbing, and the visceral resonance range is easily distinguishable in a ride simulator which is driven slowly through this frequency range.

27. In order to determine the feasibility of measuring magnitudes of accelerations in such a way that they could be correlated with subjective judgments of ride quality, five people were driven over 21 separate paved roads and unimproved trails at the Chrysler Chelsea Proving Grounds in two different wheeled vehicles (M37, 4x4 3/4-ton truck, and the XM410, 8x8 2-1/2-ton truck). Judgments of the ride quality were obtained from each person for each road section in each vehicle. Time recordings of the vibratory accelerations along three perpendicular axes were obtained at the seat for each vehicle for each road section. These acceleration traces were recorded on magnetic tape and converted with an analog computer into statistical quantities suitable for analysis. The subjective judgments were compared with the physical quantities derived from the acceleration recordings. This correlation constituted the major objective of this investigation and was performed with a digital computer.

28. Table A is a summary of some of the correlation coefficients from this study.

Table A

Correlation Coefficients Between Ride and RMS Acceleration

Criterion		M37	XM410	Both Vehicles
Dieckmann	Vertical	.683	.830	.774
	Transverse	.803	.849	.426
	Fore & Aft	.579	.887	.619
Van Deusen	Vertical	.483	.895	.787
	Transverse	.377	.817	.447
	Fore & Aft	.393	.880	.640

29. Table A shows correlation coefficients between ride and root mean square (rms) acceleration. Two different criteria are compared in this table. The Dieckmann criterion emphasized low frequencies and the Van Deusen criterion emphasized the area associated with the visceral resonance. The largest correlation coefficient found in this study was .895 for the XM410 using the Van Deusen criterion. There is a considerable difference between the correlation found in the M37 vehicle and the XM410 vehicle. The frequency distribution is determined by the vehicle configuration, i.e. the road or terrain input has no predominant frequency components and, therefore, the natural resonance frequencies of the vehicle determine the frequency content of the vibration. This is probably the reason for the rather large difference in correlation coefficients for the two vehicles. It is suggested that a single number (properly filtered rms acceleration) derived from actual acceleration measurements may be a meaningful ride index for a given vehicle, but to compare ride for a number of vehicle configurations, it is necessary to have more than one number to characterize the vibration.

30. Conclusions reached from the review of the state of the art and the feasibility study are as follows:

a. It is clear that the problem of correlating acceleration values with subjective ride sensation is an extremely difficult one. The feasibility study however indicated that rms acceleration can be correlated with subjective response of a ride jury.

b. No single number obtained by averaging the entire frequency spectrum provides an adequate description of ride. This is due to the number of different sensing mechanisms involved in the ride evaluation and to the fact that these sensing mechanisms are frequency dependent; they thus "color" the judgment of ride quality. A correlation of the square of the acceleration in each of the basic low frequency bands with subjective response should give meaningful ride criteria and determine the relations between acceleration variance and ride sensation.

c. It has also been concluded that human response can be predicted from acceleration variance as a function of frequency for steady state vibration excited by stable ground roughness.

Theoretical dynamic aspects of vehicle systems

31. The theoretical dynamics aspects of the problem are concerned with the verification and development of mathematical models of the vibrational response of vehicles. Although the modeling methods are well established, considerable work is required before acceptable agreement can be achieved between actual and predicted results.

32. The problem of defining representative models for vehicle systems has been studied by many investigators for many years. Most of the publications in this area pertain to model design to answer specific problems. The literature can be divided into two different categories:

a. Attempts to subject models to artificial inputs and to validate the resulting prediction by constructing a similar input for the vehicle.

b. Attempts to define the inputs statistically and analyze the behavior of these models.

33. Most of the early analyses pertain to deterministic inputs, such as step functions or sine waves, and describe the response of a vehicle system to these inputs. The method of analysis used is either an analog computer simulation of the system or an analysis in the frequency domain using transfer functions calculated for the linear vehicle system. While deterministic inputs have yielded direct computer response time traces, there is in the literature no available information on statistical outputs calculated for cross-country military vehicles. A

number of airplane structures have been analyzed statistically and the methods employed are of general interest in this study. Two problems exist in the interpretation of previous experiments in the present context.

a. Only linear systems have been used as models for the statistical methods of analysis. Some nonlinearities in the vehicle dynamic systems are pertinent to the analysis and must be included.

b. All vehicle models reported in the literature include only a vertical input. It is noted from vibration recordings in an actual vehicle that the fore and aft vibration can be equal to, and in some cases larger than, the vertical vibration.

34. The previous methods of computer modeling have been extended to allow direct interpretation in terms of random vibration. This extension is primarily one of defining the input and interpreting the output. The models used are similar to those in the literature. Two different methods of modeling were used in different portions of the study. The first is a time domain analysis which will allow a direct prediction of the output power spectral density, and, if necessary cross spectral densities, for a nonlinear system. The second is a digital computer program which produces the same results for a more detailed, but linear, system with the computation performed in the frequency domain.

35. A feasibility study of a linear vehicle model of the M37 vehicle was chosen for analysis using both of the techniques described. Fig. 23 shows a measured power spectral density for the M37 vehicle in cross-country operation. Fig. 24 shows the output acceleration power spectral density predicted using the frequency domain approach, with a constant-level velocity input. Fig. 25 shows the output power spectral density, calculated from the time domain approach, for the same system with only one rear wheel excited. These three curves indicate that the two predictions of the computer model output have essentially three peaks. The lowest peak is due to the bounce motion of the vehicle, and the second peak is due to the combination of the pitch and roll motions of the vehicle. The third peak at approximately 7.5 cps is a combination of all wheel hop motions of the vehicle, i.e. the bounce and roll motions of both axle assemblies. These same peaks can be seen in fig. 23 together with some secondary peaks which might be attributed to second harmonics resulting

from nonlinearities in the system. Comparison of these graphs shows that the frequency of the peaks and the ratio of amplitude compare quite well for the two different computer model analyses and for the measured vehicle response.

36. The conclusions made on the basis of the literature review, the development of the modeling techniques, and the example of the use of these techniques are as follow:

a. Although the model may have been oversimplified for the analysis used in the example, it definitely shows the feasibility of using these modeling techniques for analysis of vehicle vibration and prediction of power spectral density for interpretation using subjective criteria.

b. The time domain approach is valid for comparison of general vehicle configurations. Thus, by treating the vehicle body as a rigid mass and analyzing only the general suspension system configuration, we can study the differences between major vehicle configurations. The frequency range of interest is approximately that from 0.5 to 10 cps (i.e. to a frequency above wheel hop resonance). While this type of analysis is most general from the standpoint of including nonlinearities, etc., it is limited in degrees of freedom from the standpoint of available analog computing facilities in most installations, and digital solution of the nonlinear equations in the time domain is difficult and time consuming when the system becomes very large.

c. The digital computer approach for analysis in the frequency domain can be used specifically for areas of vehicle design where more detail is needed in the model. While the model must be linear, it is useful for determining the significance of attachment points of various suspension elements, suspension geometry considerations, etc. The frequency range of interest is from approximately 0.5 to 25 cps and this model will, in general, include the power plant assembly, the seat on its mounting system, the fundamental bending and torsional modes of the vehicle frame structure, and detail of the suspension systems. This type of model can be easily incorporated on many existing digital computers.

d. No solution has been offered to the fore and aft input to the wheel, and it is strongly urged that development be initiated to define a pertinent input of this nature. It is not difficult to include the pertinent degrees of freedom in the computer models once the input is defined.

Terrain measurements

37. The theoretical dynamics aspect of this study defines the measurement of terrain profile necessary for analysis of vehicle systems. For the frequency domain approach, it was found that the power spectral density of the profile between each pair of wheels was necessary as an input. In the time domain, a continuous time trace of the profile is necessary; and, in reality, it should be two time traces separated (in measurement) by the tread width of the vehicle. To accomplish these measurements, a brief review of the characteristics of the measuring devices available was made. It appears from the above criteria that each profile should be measured as a continuous analog function and recorded separately on two tracks of a tape recorder, which would allow simultaneous playback of both signals. The power spectral density and cross spectral density statistics can be used as inputs for the frequency domain portion of this analysis and will permit a convenient method of comparing different terrain profiles in a statistical sense. For the time domain program, including nonlinearities, it is necessary to use the actual terrain profile.

38. A survey of the existing devices to measure terrain geometry was made. The methods identified in the literature can be divided into three general categories: (a) profilometers; (b) roughmeters; and (c) rod and transit. The first two are automatic mechanical-electrical devices, whereas the last device is manually operated.

a. Profilometers provide continuous graphic profiles using a moving average reference plane formed by the wheels of the vehicle carrying the profilometer. The measurement is between this plane and a single profile measuring wheel. The geometry of the road wheel precludes measurement of frequencies below a certain wavelength.

b. Roughmeters are similar to the profilometer except that the continuous graphic profile is obtained from a wheel assembly which acts as a seismic device. By measuring the difference in displacement between the bed of the carrying device and the wheel assembly forming the seismic device, it is possible to record continuously the terrain profile.

c. Rod and transit method employs conventional surveying techniques. While slow, tedious, and expensive, it is the only method for achieving the necessary level of accuracy for defining terrain profiles.

39. It has been concluded on the basis of this study that the only presently available method of obtaining accurate terrain profile data suitable for analysis of vehicle systems is the slow and expensive rod and transit method. It is suggested that a device acceptable for measuring terrain profiles automatically should be capable of measuring ground wavelengths between 0.011 and 2.73 cycles per foot as a continuous analog recording of two tracks.

Conclusions

40. As might have been expected, the two approaches to the problem of describing and defining the dynamic response characteristics have not led to a clear judgment of the superiority of one over the other. They have, however, forced the schools of thought to shift their ground slightly. The FMC approach, which traces force and motion in real time through the vehicle suspension system, has been demonstrated to be a useful design tool. In fact, the FMC Corporation is currently using it to design the suspension system of its new armored personnel carrier, and it appears safe to predict that the new machine will be a substantial improvement over the M113. The force-motion system does not, of course, yield a description of ride which can be readily correlated with human response. For this, the Chrysler Corporation statistical system appears to be the only solution in sight.

41. Thus, it appears that the dual approach has revealed, among other things, that there are two separate and distinct problems instead of one as had been previously assumed. One problem is to define force and motion in a suspension system in such a way that the relations can be used to improve the design of suspension systems. This the FMC

Corporation mathematical model appears to do. The other problem is to describe motion in objective terms in such a way that the mathematically derived terms correlate directly with human response. While a satisfactory solution to this problem has not yet been achieved, it appears that the Chrysler Corporation statistical procedure will be suitable for this purpose.

Table 1

Deflections and Deflection Rates Used in Vehicle Model

TIRE DEFLECTIONS:

$$\delta_1 = XX_1 - X_{12} - \frac{l}{2}\phi_{12}$$

$$\delta_2 = XX_2 - X_{12} + \frac{l}{2}\phi_{12}$$

$$\delta_3 = XX_3 - X_{34} + \frac{l}{2}\phi_{34}$$

$$\delta_4 = XX_4 - X_{34} - \frac{l}{2}\phi_{34}$$

SUSPENSION DEFLECTIONS:

$$\Delta_1 = \bar{X} + l l_f \theta - \frac{l_f}{2}\gamma + X_{12} + \frac{l_f}{2}\phi_{12}$$

$$\Delta_2 = \bar{X} + l l_f \theta + \frac{l_f}{2}\gamma + X_{12} - \frac{l_f}{2}\phi_{12}$$

$$\Delta_3 = \bar{X} - l l_r \theta + \frac{l_r}{2}\gamma + X_{34} - \frac{l_r}{2}\phi_{34}$$

$$\Delta_4 = \bar{X} - l l_r \theta - \frac{l_r}{2}\gamma + X_{34} + \frac{l_r}{2}\phi_{34}$$

TIRE DEFLECTION RATES:

$$\dot{\delta}_1 = \dot{X}\dot{X}_1 - \dot{X}_{12} - \frac{l}{2}\dot{\phi}_{12}$$

$$\dot{\delta}_2 = \dot{X}\dot{X}_2 - \dot{X}_{12} + \frac{l}{2}\dot{\phi}_{12}$$

$$\dot{\delta}_3 = \dot{X}\dot{X}_3 - \dot{X}_{34} + \frac{l}{2}\dot{\phi}_{34}$$

$$\dot{\delta}_4 = \dot{X}\dot{X}_4 - \dot{X}_{34} - \frac{l}{2}\dot{\phi}_{34}$$

SUSPENSION DEFLECTION RATES:

$$\dot{\Delta}_1 = \dot{\bar{X}} + l l_f \dot{\theta} - \frac{l_f}{2}\dot{\gamma} + \dot{X}_{12} + \frac{l_f}{2}\dot{\phi}_{12}$$

$$\dot{\Delta}_2 = \dot{\bar{X}} + l l_f \dot{\theta} + \frac{l_f}{2}\dot{\gamma} + \dot{X}_{12} - \frac{l_f}{2}\dot{\phi}_{12}$$

$$\dot{\Delta}_3 = \dot{\bar{X}} - l l_r \dot{\theta} + \frac{l_r}{2}\dot{\gamma} + \dot{X}_{34} - \frac{l_r}{2}\dot{\phi}_{34}$$

$$\dot{\Delta}_4 = \dot{\bar{X}} - l l_r \dot{\theta} - \frac{l_r}{2}\dot{\gamma} + \dot{X}_{34} + \frac{l_r}{2}\dot{\phi}_{34}$$

Table 2
Equations of Motion for 4-Wheel Vehicle

BODY BOUNCE EQUATION:

$$(-K_1-K_2)X_{12}+(-C_1-C_2)\dot{X}_{12}+(-K_3-K_4)X_{34}+(-C_3-C_4)\dot{X}_{34}$$
$$+(-K_1+K_2)\frac{l_f}{2}\phi_{12}+(-C_1+C_2)\frac{l_f}{2}\dot{\phi}_{12}+(K_3-K_4)\frac{l_r}{2}\phi_{34}$$
$$+(C_3-C_4)\frac{l_r}{2}\dot{\phi}_{34}+(-K_1-K_2-K_3-K_4)\bar{X}+(-C_1-C_2-C_3-C_4)\dot{\bar{X}}-\frac{W}{g}\ddot{\bar{X}}$$
$$+\left[(-K_1-K_2)l l_f+(K_3+K_4)l l_r\right]\theta+\left[(-C_1-C_2)l l_f+(C_3+C_4)l l_r\right]\dot{\theta}$$
$$+\left[(K_1-K_2)\frac{l_f}{2}+(-K_3+K_4)\frac{l_r}{2}\right]\gamma+\left[(C_1-C_2)\frac{l_f}{2}+(-C_3+C_4)\frac{l_r}{2}\right]\dot{\gamma}=0$$

BODY PITCH EQUATION:

$$(-K_1-K_2)l l_f X_{12}+(-C_1-C_2)l l_f\dot{X}_{12}+(K_3+K_4)l l_r X_{34}$$
$$+(C_3+C_4)l l_r\dot{X}_{34}+(-K_1+K_2)l l_f\frac{l_f}{2}\phi_{12}+(-C_1+C_2)l l_f\frac{l_f}{2}\dot{\phi}_{12}$$
$$+(-K_3+K_4)l l_r\frac{l_r}{2}\phi_{34}+(-C_3+C_4)l l_r\frac{l_r}{2}\dot{\phi}_{34}$$
$$+\left[(-K_1-K_2)l l_f+(K_3+K_4)l l_r\right]\bar{X}+\left[(-C_1-C_2)l l_f+(C_3+C_4)l l_r\right]\dot{\bar{X}}$$
$$+\left[(-K_1-K_2)(l l_f)^2+(-K_3-K_4)(l l_r)^2\right]\theta+\left[(-C_1-C_2)(l l_f)^2+(-C_3-C_4)(l l_r)^2\right]\dot{\theta}$$
$$-\bar{I}_Y\ddot{\theta}+\left[(K_1-K_2)l l_f\frac{l_f}{2}+(K_3-K_4)l l_r\frac{l_r}{2}\right]\gamma$$
$$+\left[(C_1-C_2)l l_f\frac{l_f}{2}+(C_3-C_4)l l_r\frac{l_r}{2}\right]\dot{\gamma}=0$$

BODY ROLL EQUATION:

$$(K_1-K_2)\frac{l_f}{2}X_{12}+(C_1-C_2)\frac{l_f}{2}\dot{X}_{12}+(-K_3+K_4)\frac{l_r}{2}X_{34}+(-C_3+C_4)\frac{l_r}{2}\dot{X}_{34}$$
$$+(K_1+K_2)\left(\frac{l_f}{2}\right)^2\phi_{12}+(C_1+C_2)\left(\frac{l_f}{2}\right)^2\dot{\phi}_{12}+(K_3+K_4)\left(\frac{l_r}{2}\right)^2\phi_{34}$$
$$+(C_3+C_4)\left(\frac{l_r}{2}\right)^2\dot{\phi}_{34}+\left[(K_1-K_2)\frac{l_f}{2}+(-K_3+K_4)\frac{l_r}{2}\right]\bar{X}$$
$$+\left[(C_1-C_2)\frac{l_f}{2}+(-C_3+C_4)\frac{l_r}{2}\right]\dot{\bar{X}}+\left[(K_1-K_2)\frac{l_f}{2}l_{l_f}+(K_3-K_4)\frac{l_r}{2}l_{l_r}\right]\theta$$
$$+\left[(C_1-C_2)\frac{l_f}{2}l_{l_f}+(C_3-C_4)\frac{l_r}{2}l_{l_r}\right]\dot{\theta}+\left[(-K_1-K_2)\left(\frac{l_f}{2}\right)^2+(-K_3-K_4)\left(\frac{l_r}{2}\right)^2\right]\gamma$$
$$+\left[(-C_1-C_2)\left(\frac{l_f}{2}\right)^2+(-C_3-C_4)\left(\frac{l_r}{2}\right)^2\right]\dot{\gamma}-\bar{I}_z\ddot{\gamma}=0$$

FRONT DIFFERENTIAL BOUNCE EQUATION:

$$KK_1XX_1+CC_1\dot{X}X_1+KK_2XX_2+CC_2\dot{X}X_2+(-KK_1-KK_2-K_1-K_2)X_{12}$$
$$+(-CC_1-CC_2-C_1-C_2)\dot{X}_{12}-\frac{W_{12}}{g}\ddot{X}_{12}+\left[(-KK_1+KK_2)\frac{l}{2}+(-K_1+K_2)\frac{l_f}{2}\right]\phi_{12}$$
$$+\left[(-CC_1+CC_2)\frac{l}{2}+(-C_1+C_2)\frac{l_f}{2}\right]\dot{\phi}_{12}+(-K_1-K_2)\bar{X}+(-C_1-C_2)\dot{\bar{X}}$$
$$+(-K_1-K_2)l_{l_f}\theta+(-C_1-C_2)l_{l_f}\dot{\theta}+(K_1-K_2)\frac{l_f}{2}\gamma$$
$$+(C_1-C_2)\frac{l_f}{2}\dot{\gamma}=0$$

FRONT DIFFERENTIAL ROLL EQUATION:

$$KK_1\frac{l}{2}XX_1+CC_1\frac{l}{2}\dot{X}X_1-KK_2\frac{l}{2}XX_2-CC_2\frac{l}{2}\dot{X}X_2$$
$$+\left[(-KK_1+KK_2)\frac{l}{2}+(-K_1+K_2)\frac{l_f}{2}\right]X_{12}+\left[(-CC_1+CC_2)\frac{l}{2}+(-C_1+C_2)\frac{l_f}{2}\right]\dot{X}_{12}$$
$$+\left[(-KK_1-KK_2)\left(\frac{l}{2}\right)^2+(-K_1-K_2)\left(\frac{l_f}{2}\right)^2\right]\phi_{12}+\left[(-CC_1-CC_2)\left(\frac{l}{2}\right)^2+(-C_1-C_2)\left(\frac{l_f}{2}\right)^2\right]\dot{\phi}_{12}$$
$$-(\bar{I}_{12})_z\ddot{\phi}_{12}+(-K_1+K_2)\frac{l_f}{2}\bar{X}+(-C_1+C_2)\frac{l_f}{2}\dot{\bar{X}}+(-K_1+K_2)\frac{l_f}{2}l_{l_f}\theta$$
$$+(-C_1+C_2)\frac{l_f}{2}l_{l_f}\dot{\theta}+(K_1+K_2)\left(\frac{l_f}{2}\right)^2\gamma+(C_1+C_2)\left(\frac{l_f}{2}\right)^2\dot{\gamma}=0$$

REAR DIFFERENTIAL BOUNCE EQUATION:

$$KK_3 XX_3 + CC_3 \dot{X}X_3 + KK_4 XX_4 + CC_4 \dot{X}X_4 + (-KK_3 - KK_4 - K_3 - K_4) X_{34}$$
$$+ (-CC_3 - CC_4 - C_3 - C_4) \dot{X}_{34} - \frac{W_{34}}{g} \ddot{X}_{34} + \left[(KK_3 - KK_4)\frac{l}{2} + (K_3 - K_4)\frac{l_r}{2}\right] \phi_{34}$$
$$+ \left[(CC_3 - CC_4)\frac{l}{2} + (C_3 - C_4)\frac{l_r}{2}\right] \dot{\phi}_{34} + (-K_3 - K_4)\bar{X} + (-C_3 - C_4)\dot{\bar{X}} + (K_3 + K_4) l l_r \theta$$
$$+ (C_3 + C_4) l l_r \dot{\theta} + (-K_3 + K_4)\frac{l_r}{2}\gamma + (-C_3 + C_4)\frac{l_r}{2}\dot{\gamma} = 0$$

REAR DIFFERENTIAL ROLL EQUATION:

$$-KK_3 \frac{l}{2} XX_3 - CC_3 \frac{l}{2} \dot{X}X_3 + KK_4 \frac{l}{2} XX_4 + CC_4 \frac{l}{2} \dot{X}X_4$$
$$+ \left[(KK_3 - KK_4)\frac{l}{2} + (K_3 - K_4)\frac{l_r}{2}\right] X_{34} + \left[(CC_3 - CC_4)\frac{l}{2} + (C_3 - C_4)\frac{l_r}{2}\right] \dot{X}_{34}$$
$$+ \left[(-KK_3 - KK_4)\left(\frac{l}{2}\right)^2 + (-K_3 - K_4)\left(\frac{l_r}{2}\right)^2\right] \phi_{34} - \left(\bar{I}_{34}\right)_E \ddot{\phi}_{34}$$
$$+ \left[(-CC_3 - CC_4)\left(\frac{l}{2}\right)^2 + (-C_3 - C_4)\left(\frac{l_r}{2}\right)^2\right] \dot{\phi}_{34} + (K_3 - K_4)\frac{l_r}{2}\bar{X}$$
$$+ (C_3 - C_4)\frac{l_r}{2}\dot{\bar{X}} + (-K_3 + K_4)\frac{l_r}{2} l l_r \theta + (-C_3 + C_4)\frac{l_r}{2} l l_r \dot{\theta}$$
$$+ (K_3 + K_4)\left(\frac{l_r}{2}\right)^2 \gamma + (C_3 + C_4)\left(\frac{l_r}{2}\right)^2 \dot{\gamma} = 0$$

BODY BOUNCE

$$-\bar{X}\sum_{j=1}^{2n} K_j \;-\dot{\bar{X}}\sum_{j=1}^{2n} C_j - \theta\sum_{i=1}^{n}\sum_{j=2i-1}^{2i} k_j\, ll_i - \dot{\theta}\sum_{i=1}^{n}\sum_{j=2i-1}^{2i} C_j\, ll_i$$

$$-\gamma\sum_{j=1}^{2n} k_j l_j - \dot{\gamma}\sum_{j=1}^{2n} C_j l_j - \sum_{i=1}^{n}\sum_{j=2i-1}^{2i} \bar{X}_i K_j - \sum_{i=1}^{n}\sum_{j=2i-1}^{2i} \dot{\bar{X}}_i C_j$$

$$+\sum_{i=1}^{n}\sum_{j=2i-1}^{2i} \phi_i K_j l_j \;+\sum_{i=1}^{n}\sum_{j=2i-1}^{2i} \dot{\phi}_i C_j l_j \;=\; \ddot{\bar{X}}\,\frac{W}{g}$$

BODY PITCH

$$-\bar{X}\sum_{i=1}^{n}\sum_{j=2i-1}^{2i} K_j\, ll_i \;-\dot{\bar{X}}\sum_{i=1}^{n}\sum_{j=2i-1}^{2i} C_j\, ll_i \;-\theta\sum_{i=1}^{n}\sum_{j=2i-1}^{2i} K_j\, ll_i^2$$

$$-\dot{\theta}\sum_{i=1}^{n}\sum_{j=2i-1}^{2i} C_j\, ll_i^2 - \gamma\sum_{i=1}^{n}\sum_{j=2i-1}^{2i} K_j l_j\, ll_i - \dot{\gamma}\sum_{i=1}^{n}\sum_{j=2i-1}^{2i} C_j l_j\, ll_i$$

$$-\sum_{i=1}^{n}\sum_{j=2i-1}^{2i} \bar{X}_i K_j\, ll_i - \sum_{i=1}^{n}\sum_{j=2i-1}^{2i} \dot{\bar{X}}_i C_j\, ll_i + \sum_{i=1}^{n}\sum_{j=2i-1}^{2i} \phi_i K_j l_j\, ll_i$$

$$+\sum_{i=1}^{n}\sum_{j=2i-1}^{2i} \dot{\phi}_i C_j l_j\, ll_i \;=\; \ddot{\theta}\,\bar{I}_y$$

i TH DIFFERENTIAL BOUNCE

$$-\bar{X}\sum_{j=2i-1}^{2i} K_j \;-\dot{\bar{X}}\sum_{j=2i-1}^{2i} C_j \;-\theta\, ll_i \sum_{j=2i-1}^{2i} K_j \;-\dot{\theta}\, ll_i \sum_{j=2i-1}^{2i} C_j$$

$$-\gamma\sum_{j=2i-1}^{2i} K_j\, l_j \;-\dot{\gamma}\sum_{j=2i-1}^{2i} C_j\, l_j \;-\bar{X}_i \sum_{j=2i-1}^{2i}\left(K_j + KK_j\right)$$

$$-\dot{\bar{X}}_i \sum_{j=2i-1}^{2i}\left(C_j + CC_j\right) + \phi_i \sum_{j=2i-1}^{2i}\left(K_j l_j + KK_j L_j\right) + \dot{\phi}_i \sum_{j=2i-1}^{2i}\left(C_j l_j + CC_j L_j\right)$$

$$+\sum_{j=2i-1}^{2i} XX_j\, KK_j \;+\sum_{j=2i-1}^{2i} \dot{X}X_j\, CC_j \;=\; \ddot{\bar{X}}_i\, \frac{W_i}{g}$$

i TH DIFFERENTIAL ROLL

$$+ \bar{X} \sum_{j=2i-1}^{2i} k_j \ell_j + \dot{\bar{Y}} \sum_{j=2i-1}^{2i} c_j \ell_j + \theta \ell\ell_i \sum_{j=2i-1}^{2i} k_j \ell_j + \dot{\theta} \ell\ell_i \sum_{j=2i-1}^{2i} c_j \ell_j$$

$$+ \gamma \sum_{j=2i-1}^{2i} k_j \ell_j^2 + \dot{\gamma} \sum_{j=2i-1}^{2i} c_j \ell_j^2 + \bar{X}_i \sum_{j=2i-1}^{2i} \left(k_j \ell_j + k k_j L_j \right)$$

$$+ \dot{\bar{X}}_i \sum_{j=2i-1}^{2i} \left(c_j \ell_j + c c_j L_j \right) - \phi_i \sum_{j=2i-1}^{2i} \left(k_j \ell_j^2 + k k_j L_j^2 \right)$$

$$- \dot{\phi}_i \sum_{j=2i-1}^{2i} \left(c_j \ell_j^2 + c c_j L_j^2 \right) + \sum_{j=2i-1}^{2i} XX_j \, kK_j L_j + \sum_{j=2i-1}^{2i} \dot{XX}_j \, cC_j L_j$$

$$= \ddot{\phi}_i \; \bar{I}_{i_{\bar{x}}}$$

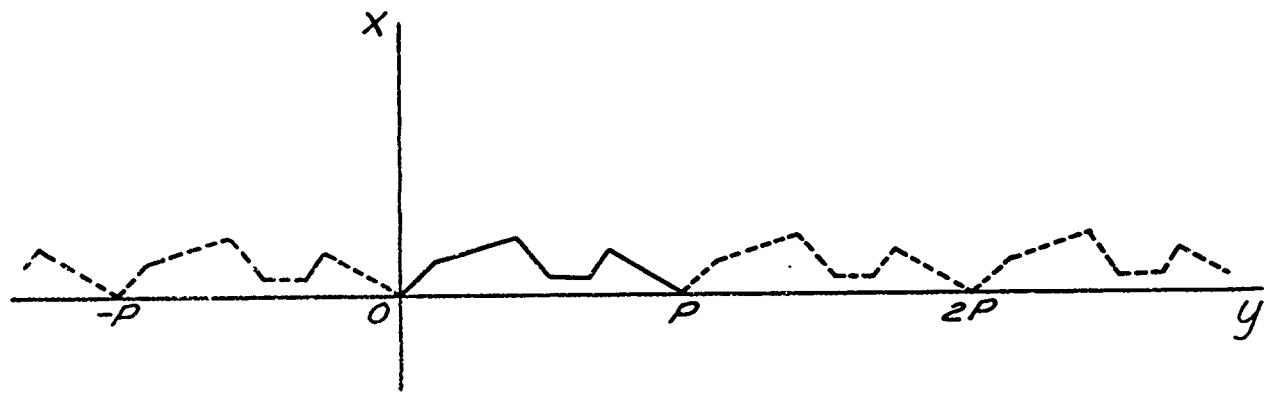

$$f(y+np) = f(y)$$

Fig. 1. Method of extending surface geometry profiles for Fourier analysis

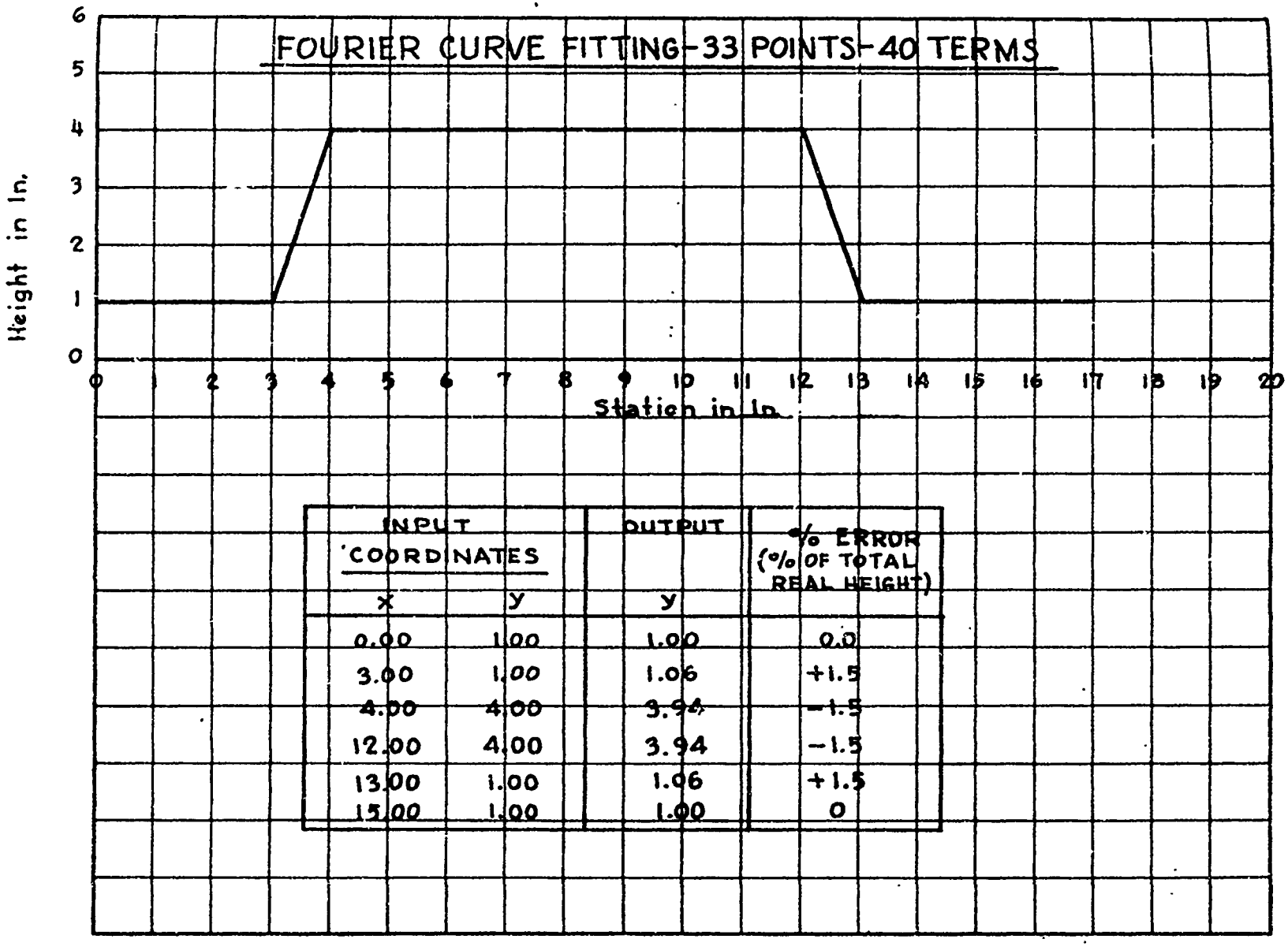

INPUT COORDINATES		OUTPUT	% ERROR (% OF TOTAL REAL HEIGHT)
x	y	y	
0.00	1.00	1.00	0.0
3.00	1.00	1.06	+1.5
4.00	4.00	3.94	−1.5
12.00	4.00	3.94	−1.5
13.00	1.00	1.06	+1.5
15.00	1.00	1.00	0

Fig. 2. Test profile used to check computer program

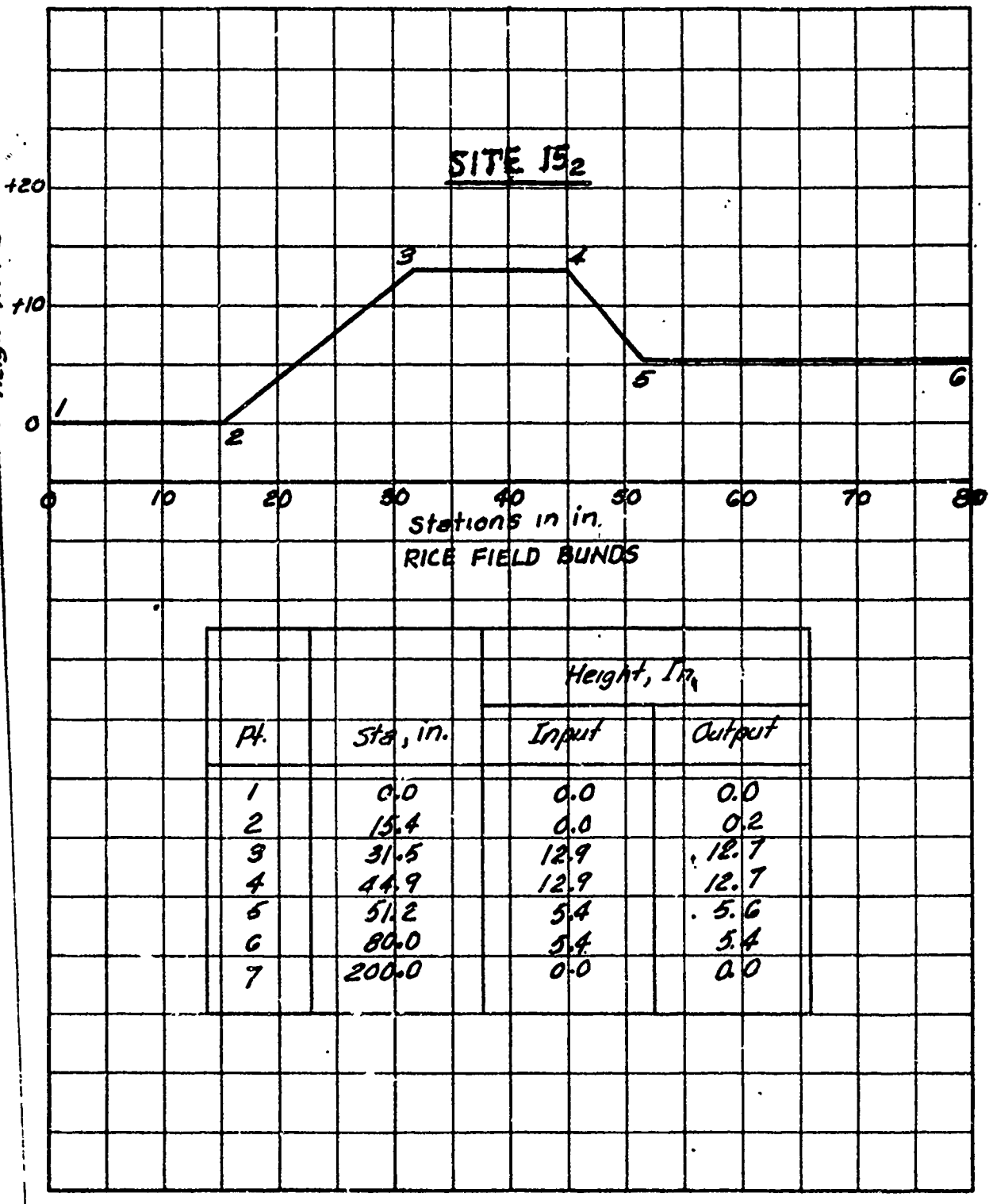

Pt.	Sta, in.	Height, In. Input	Output
1	0.0	0.0	0.0
2	15.4	0.0	0.2
3	31.5	12.9	12.7
4	44.9	12.9	12.7
5	51.2	5.4	5.6
6	80.0	5.4	5.4
7	200.0	0.0	0.0

Fig. 3. Site 15_2, rice field bund

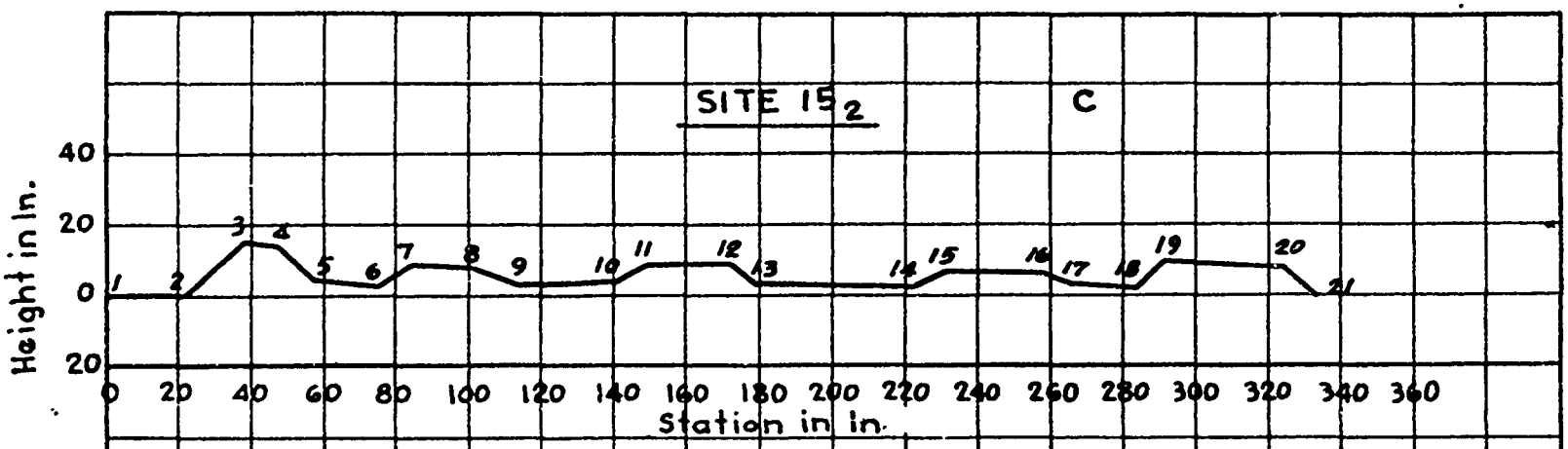

FIELD PREPARED FOR UNIDENTIFIED ROW CROP

PT.	STA, IN.	HEIGHT, IN. INPUT	HEIGHT, IN. OUTPUT	PT.	STA, IN.	HEIGHT, IN. INPUT	HEIGHT, IN. OUTPUT
1	0.0	0.0	0.3	11	149.0	9.0	8.8
2	22.0	0.0	0.3	12	172.0	9.0	8.7
3	38.0	15.0	14.7	13	178.0	3.0	3.3
4	47.0	14.0	13.8	14	232.0	3.0	3.1
5	57.0	5.0	5.3	15	231.0	7.0	6.8
6	75.0	3.0	3.3	16	258.0	7.0	6.7
7	84.0	9.0	8.7	17	266.0	3.0	3.2
8	102.0	8.0	7.9	18	283.0	2.0	2.4
9	114.0	3.0	3.1	19	291.0	10.0	9.6
10	141.0	4.0	4.2	20	324.0	9.0	8.7
				21	333.0	0.0	0.3

Fig. 4. Site 15_2. Field prepared for row crop

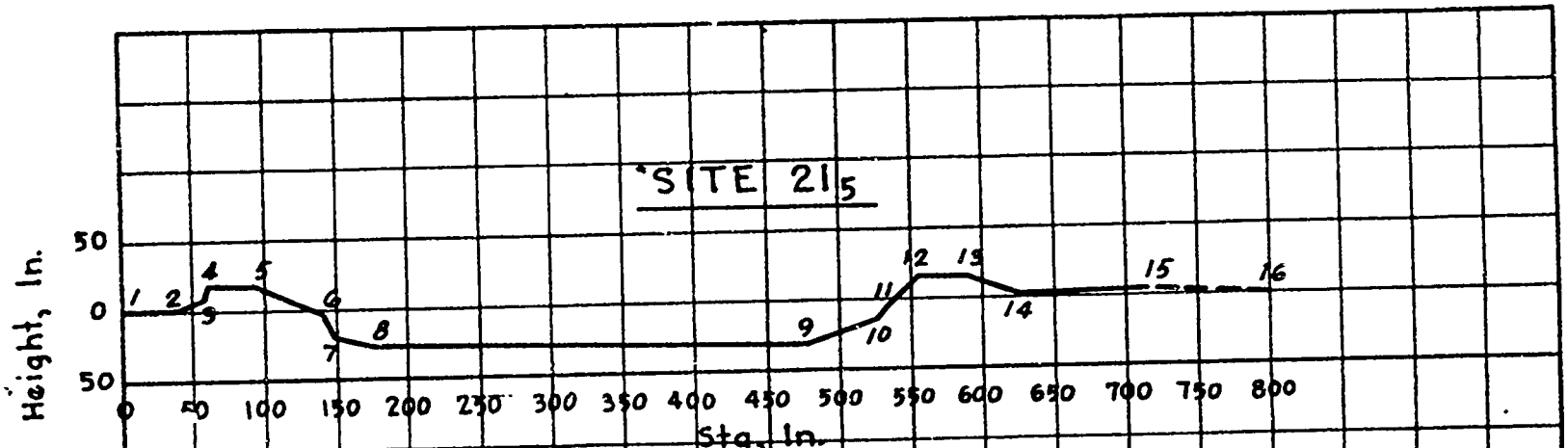

WATER CHANNEL, CANALIZED

PT	STA, IN	HEIGHT, IN. INPUT	HEIGHT, IN. OUTPUT	PT	STA, IN.	HEIGHT, IN. INPUT	HEIGHT, IN. OUTPUT
1	0	0	0.1	9	475	-31	-30.7
2	35	1	0.8	10	524	-14	-18.8
3	56	7	10.9	11	533	-3	- 3.1
4	68	18	14.0	12	554	11	16.4
5	92	17	16.8	13	587	17	16.7
6	139	-3	-4.7	14	626	2	2.3
7	146	-19	-17.2	15	715	5	4.9
8	175	-27	-26.6	16	800	0	0.1

Fig. 5. Site 21₅, canalized wate. channel

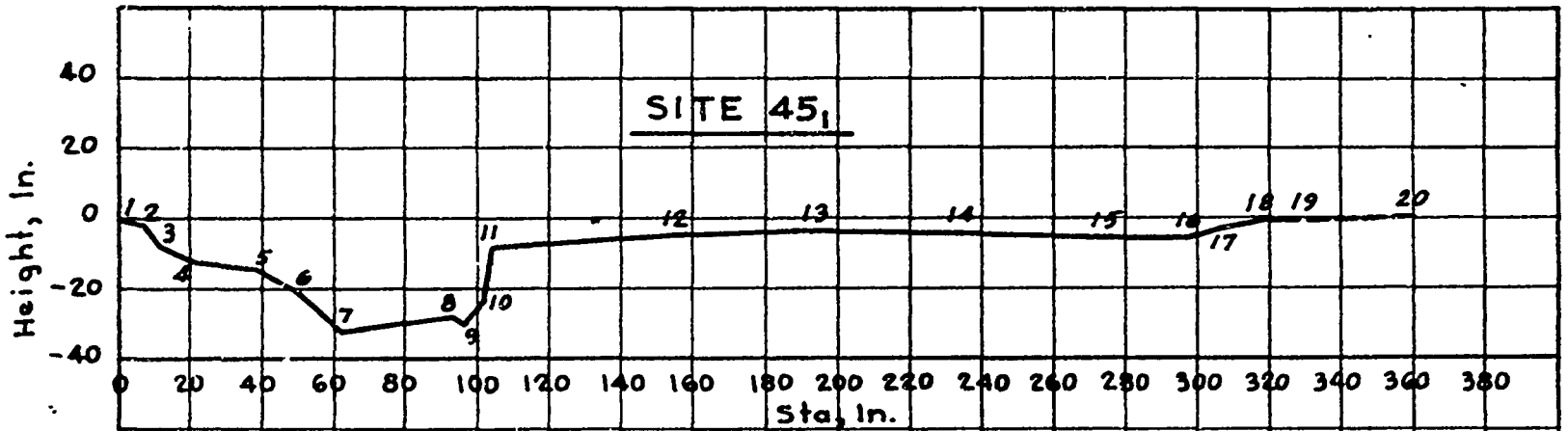

STREAM CHANNEL

PT	STA, IN	HEIGHT, IN. INPUT	HEIGHT, IN. OUTPUT	PT	STA, IN.	HEIGHT, IN. INPUT	HEIGHT, IN. OUTPUT
1	0	0	0.0	11	104	-9	-10.9
2	8	-2	-2.5	12	134	-5	-4.9
3	12	-9	-8.5	13	194	-3	-3.0
4	32	-12	-12.1	14	232	-5	-5.0
5	39	-15	-15.1	15	272	-6	-6.0
6	51	-21	-21.2	16	296	-6	-5.9
7	62	-32	-31.6	17	305	-4	-4.0
8	93	-28	-28.7	18	317	-1	-1.1
9	96	-31	-29.7	19	328	-1	-1.0
10	101	-23	-21.4	20	360	0	0.0

Fig. 6. Site 45_1, stream channel

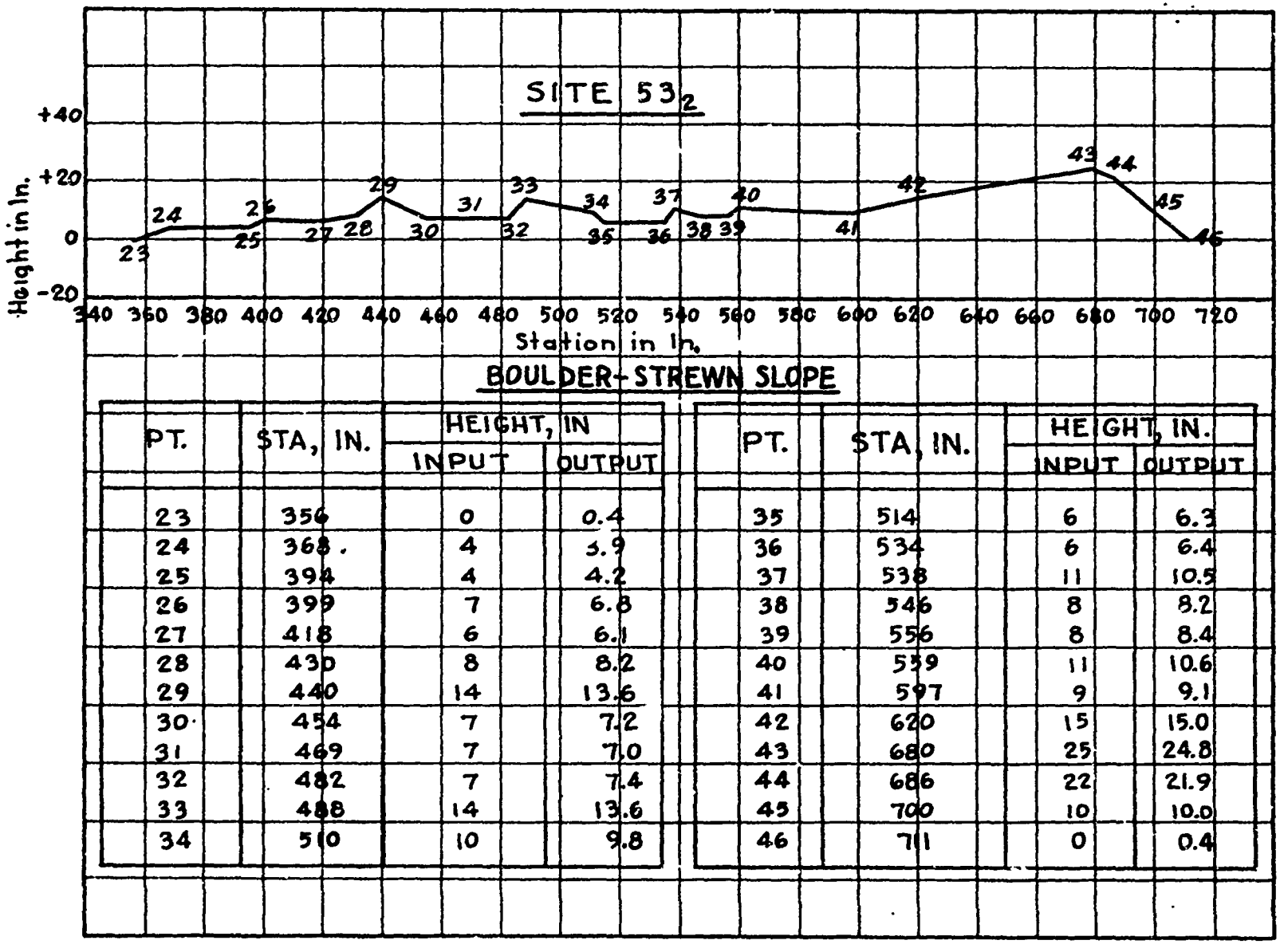

BOULDER-STREWN SLOPE

PT.	STA, IN.	HEIGHT, IN INPUT	HEIGHT, IN OUTPUT	PT.	STA, IN.	HEIGHT, IN. INPUT	HEIGHT, IN. OUTPUT
23	356	0	0.4	35	514	6	6.3
24	368	4	3.9	36	534	6	6.4
25	394	4	4.2	37	538	11	10.5
26	399	7	6.8	38	546	8	8.2
27	418	6	6.1	39	556	8	8.4
28	430	8	8.2	40	559	11	10.6
29	440	14	13.6	41	597	9	9.1
30	454	7	7.2	42	620	15	15.0
31	469	7	7.0	43	680	25	24.8
32	482	7	7.4	44	686	22	21.9
33	488	14	13.6	45	700	10	10.0
34	510	10	9.8	46	711	0	0.4

Fig. 7. Site 53_2, boulder-strewn slope

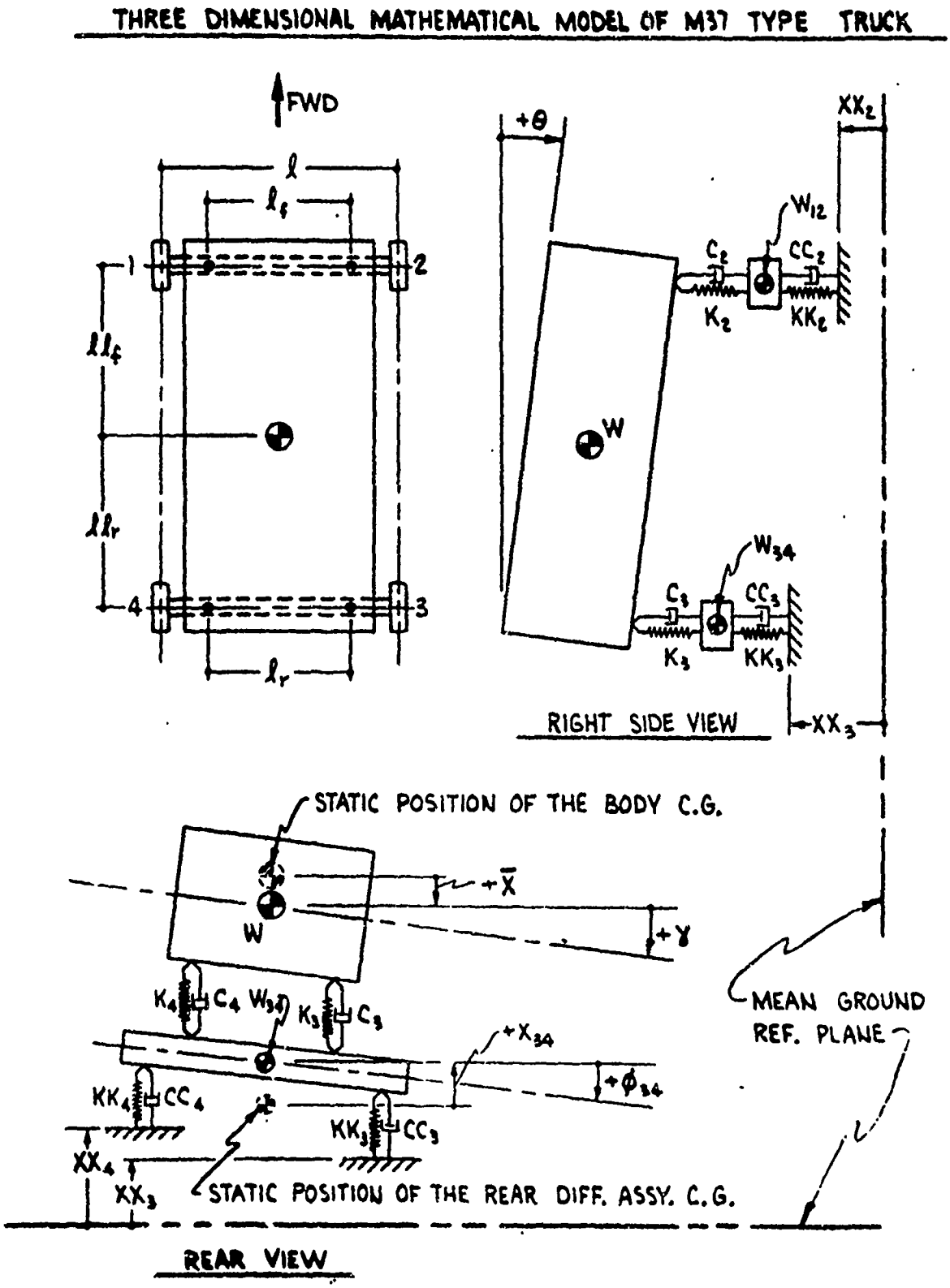

Fig. 8. Diagrammatic representation of three-dimensional mathematical model

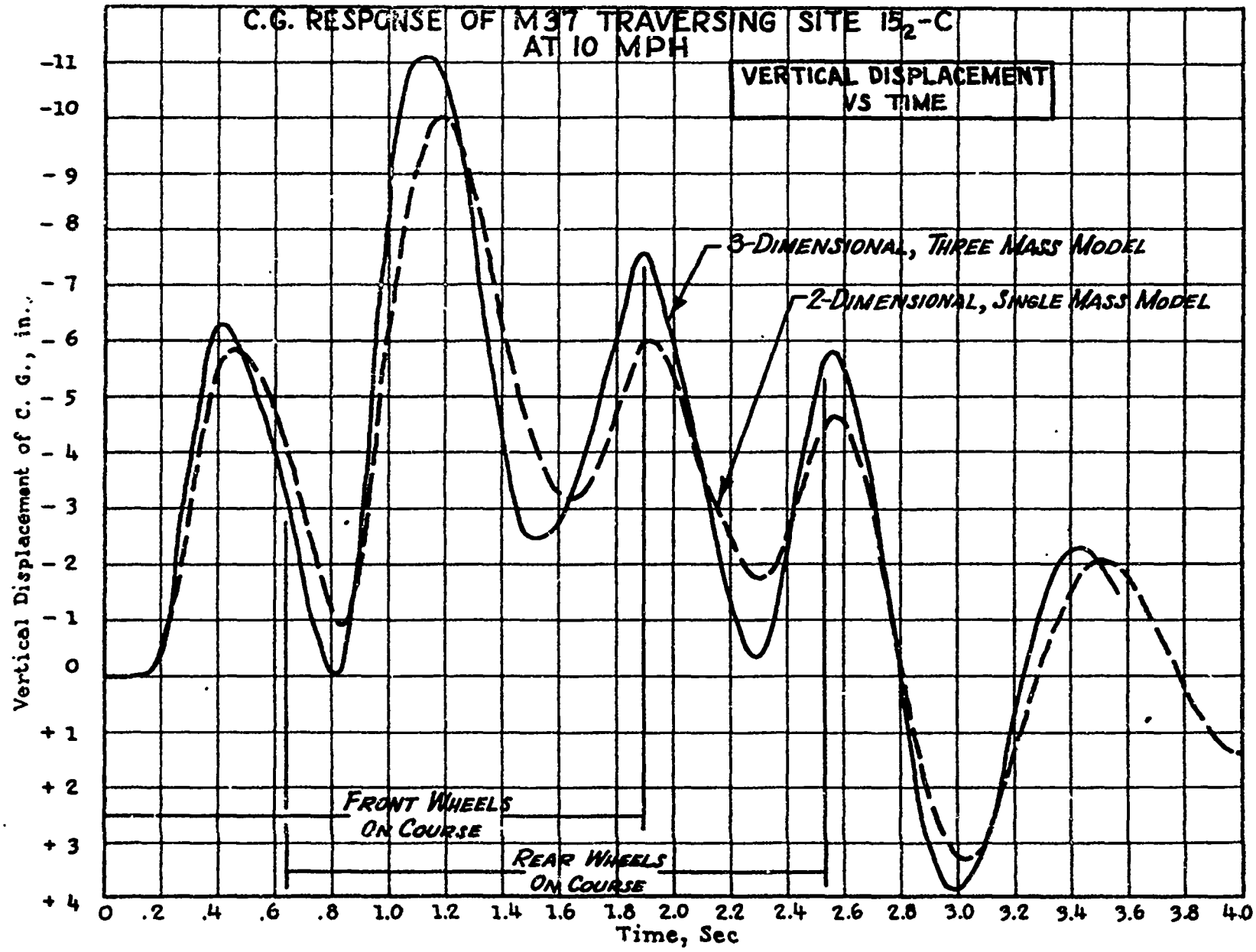

Fig. 9. Site 15_2 response, vertical displacement versus time

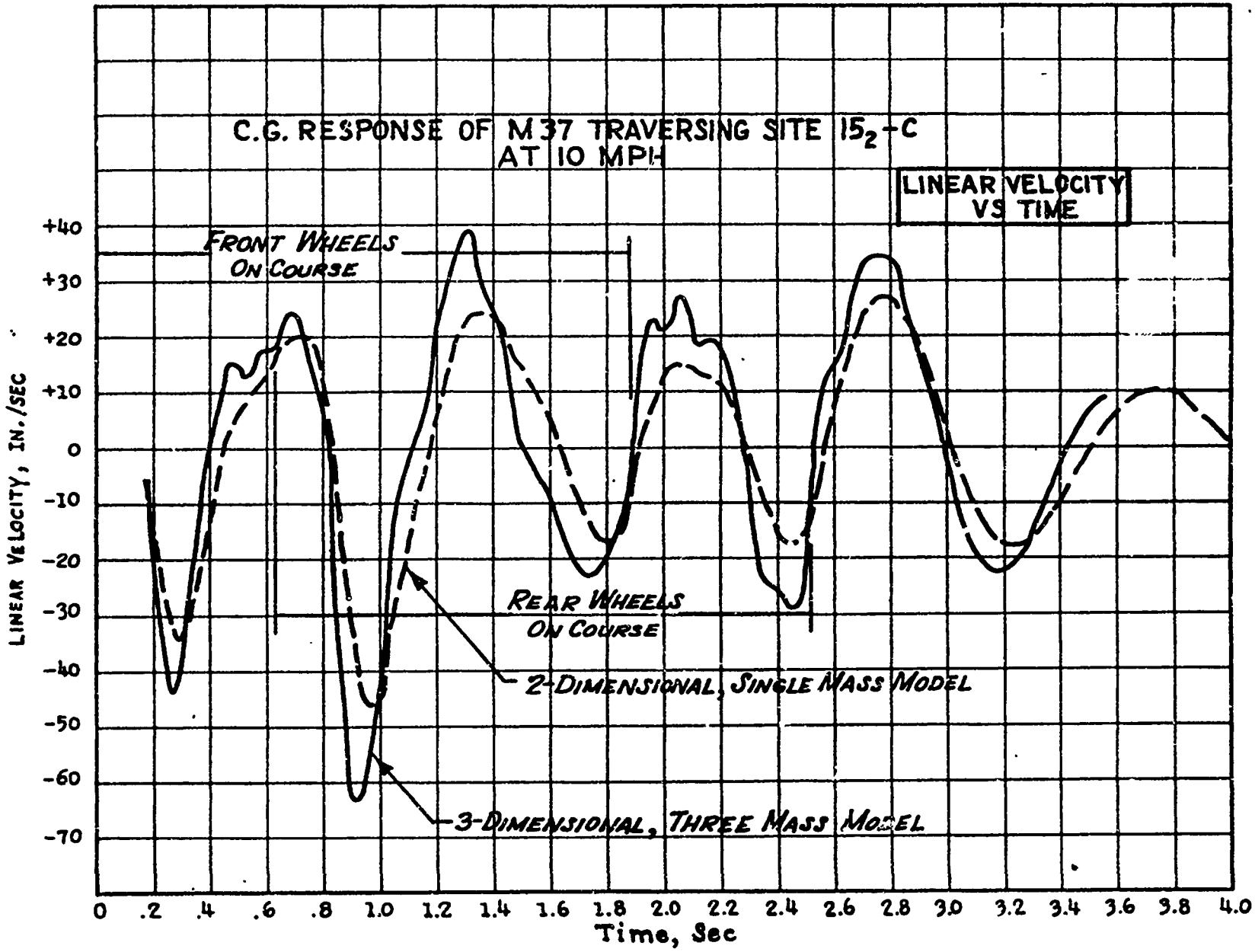

Fig. 10. Site 15_2 response, vertical velocity versus time

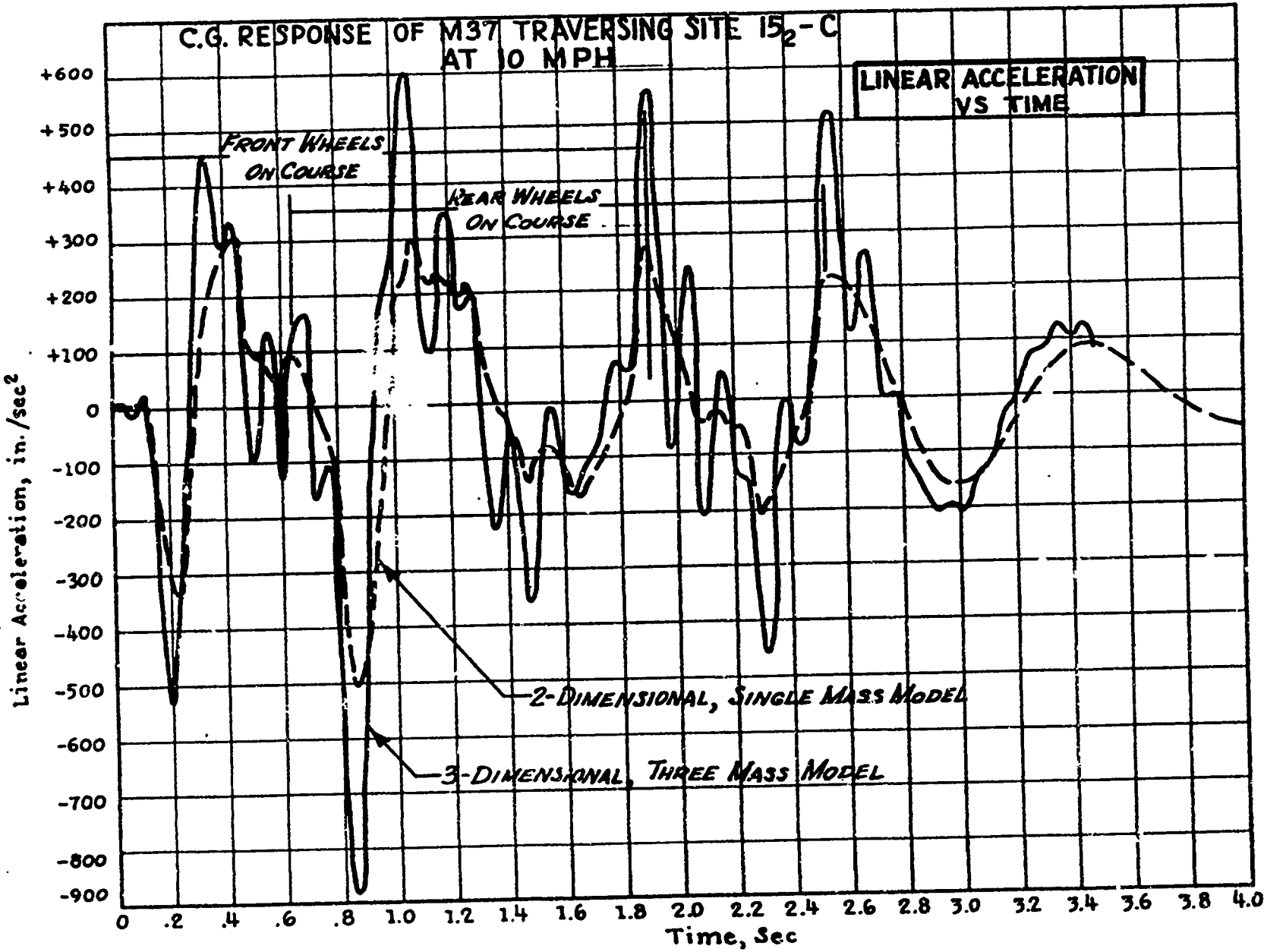

Fig. 11. Site 15_2 response linear acceleration versus time

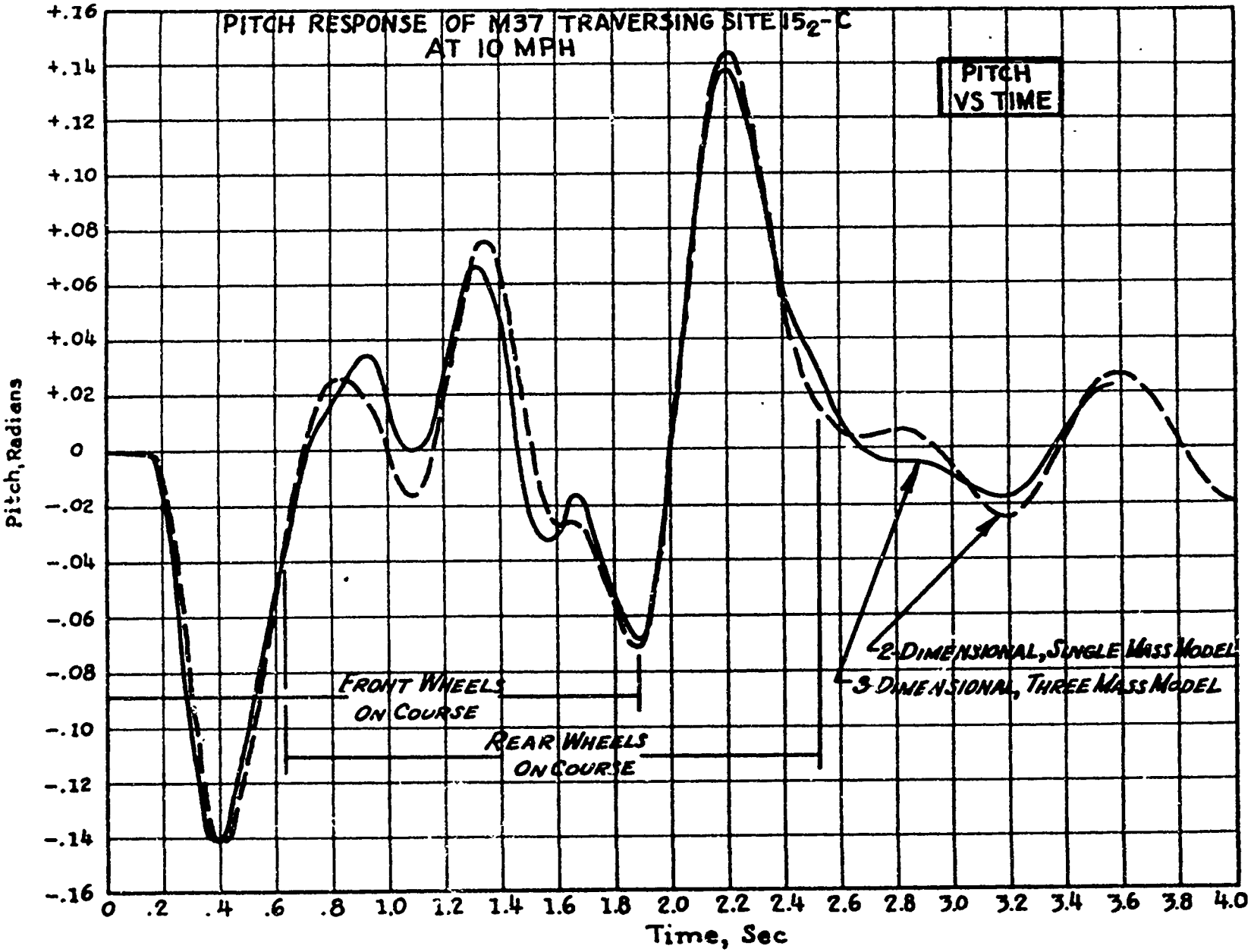

Fig. 12. Site 15_2 response, pitch displacement versus time

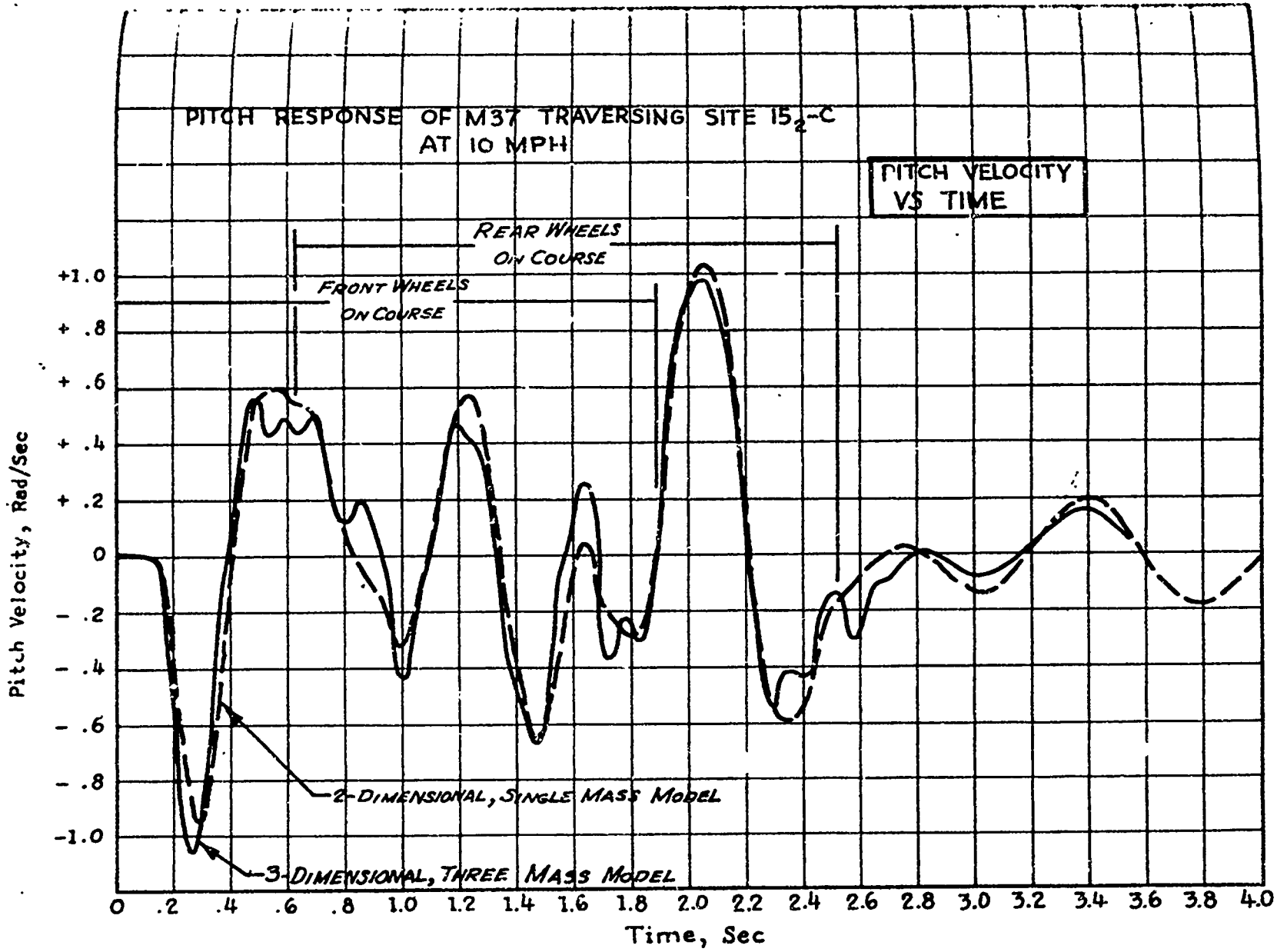

Fig. 13. Site 15_2 response, pitch velocity versus time

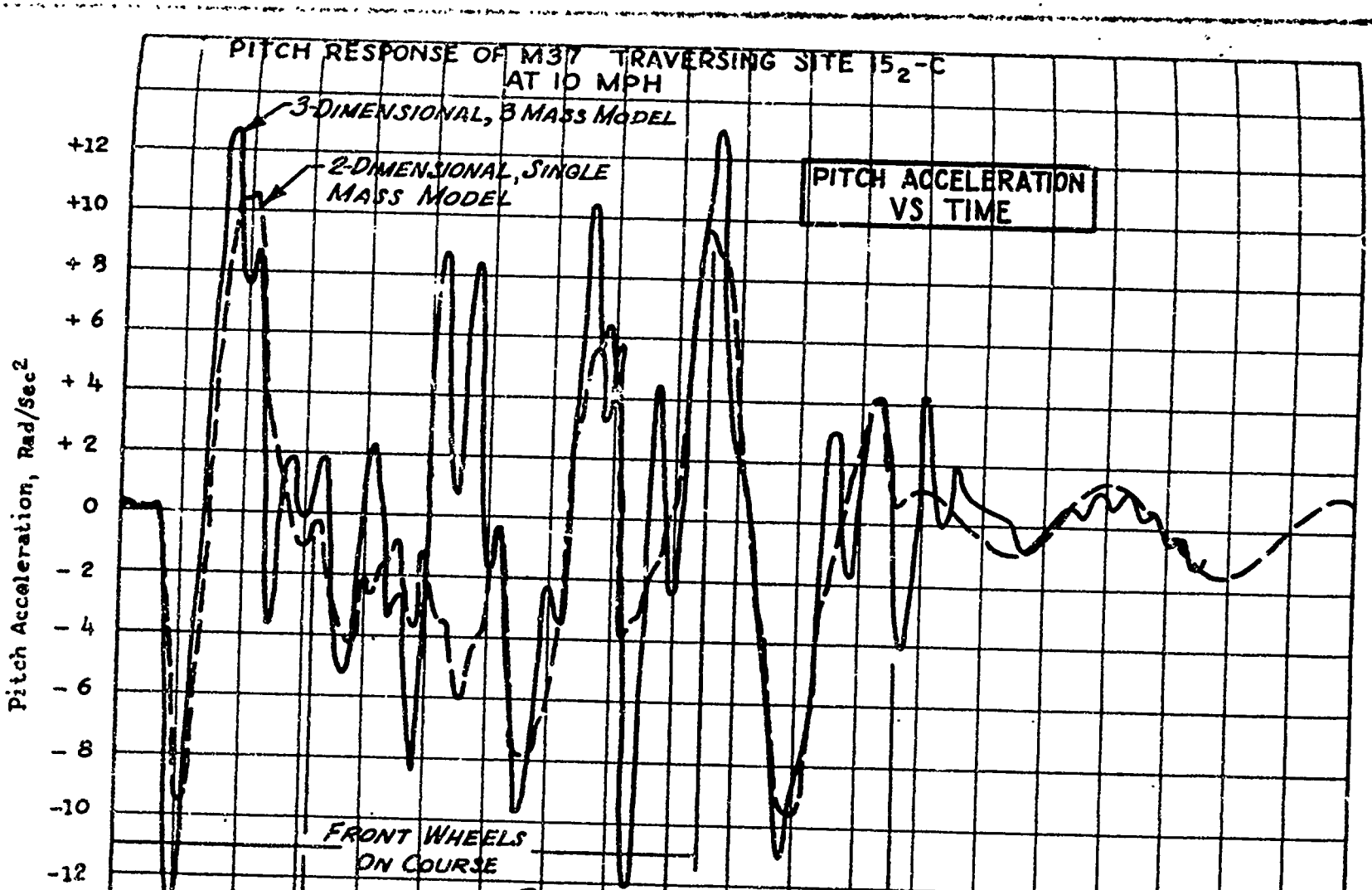

Fig. 14. Site 15_2 response, pitch acceleration versus time

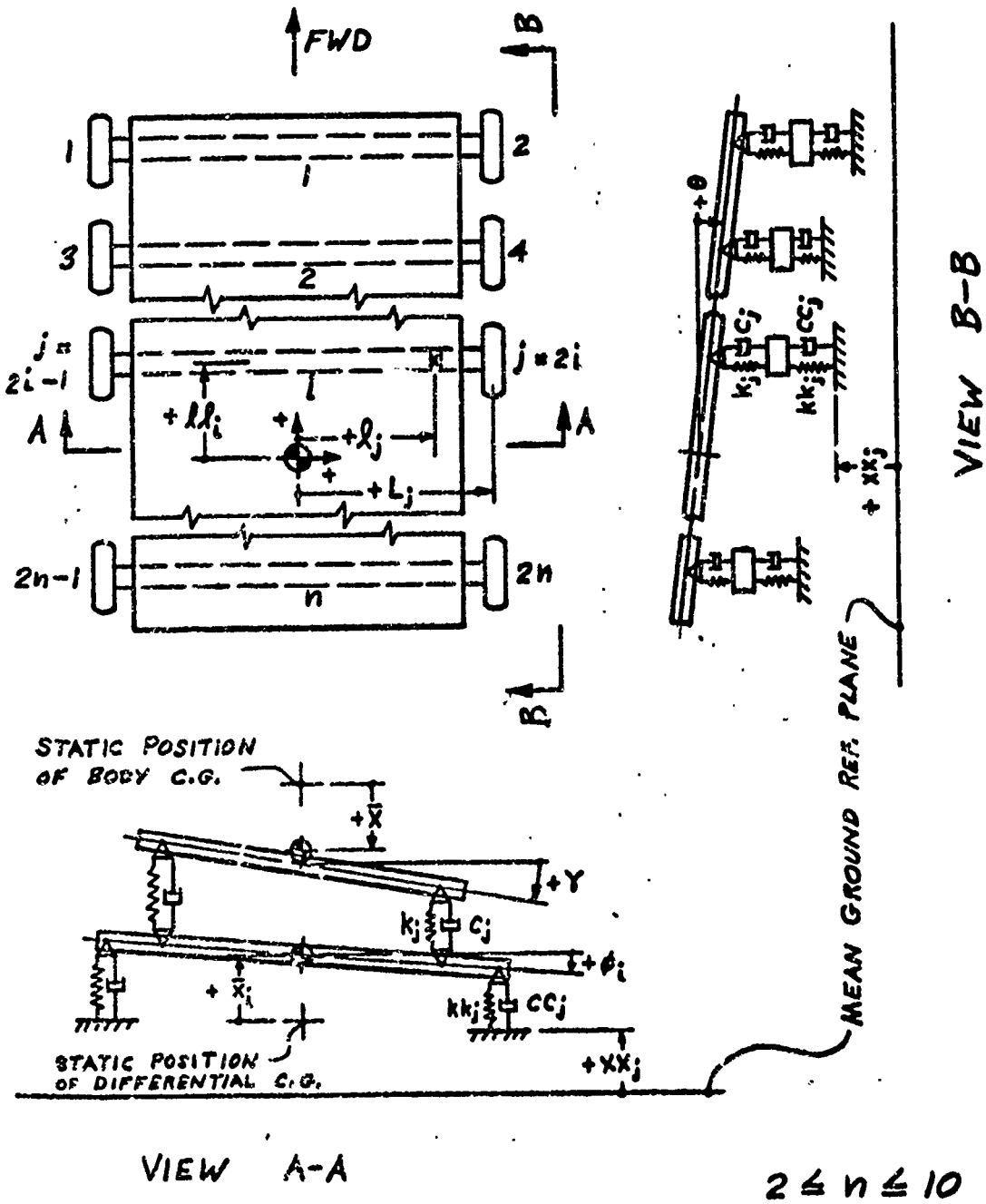

Fig. 15. Schematic of general model of wheeled vehicle

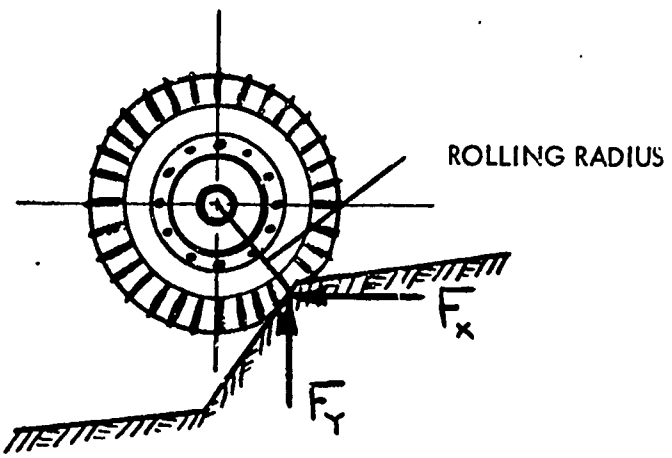

VEHICLE TIRE IMPACTING
A TERRAIN BUMP

Fig. 16

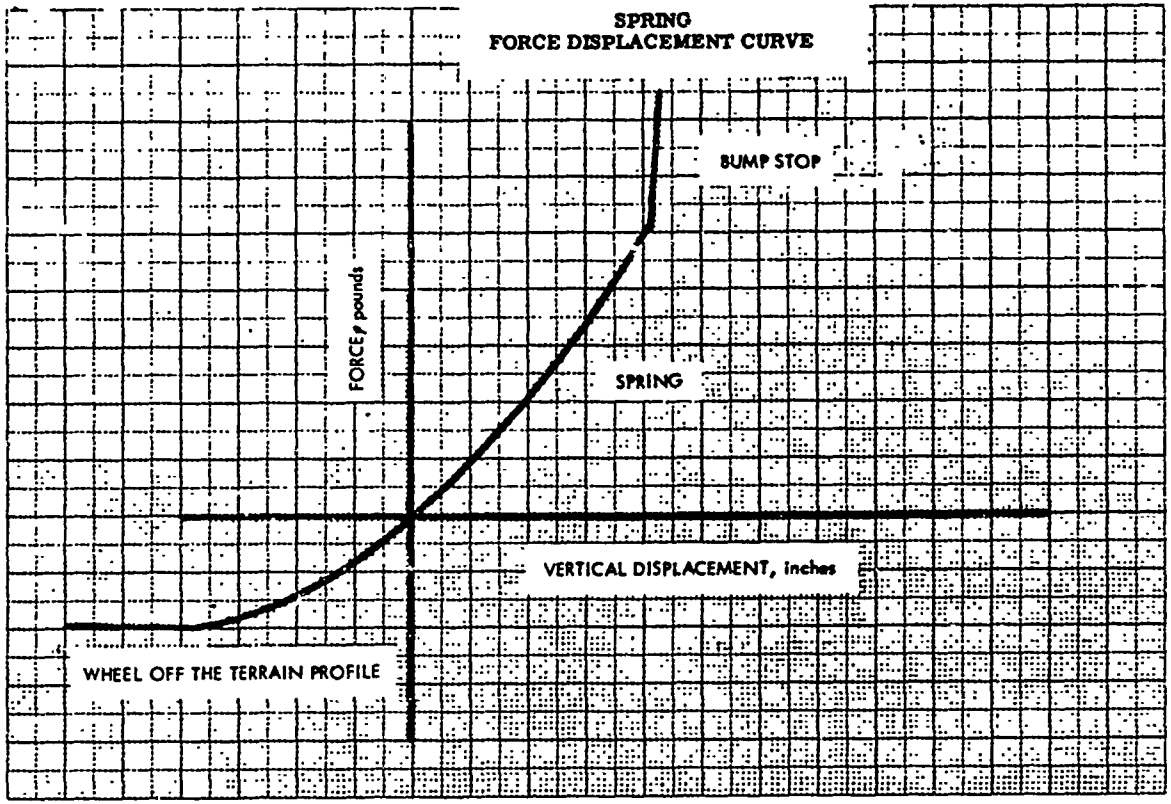
SPRING
FORCE DISPLACEMENT CURVE
BUMP STOP
FORCE, pounds
SPRING
VERTICAL DISPLACEMENT, inches
WHEEL OFF THE TERRAIN PROFILE

Fig. 17

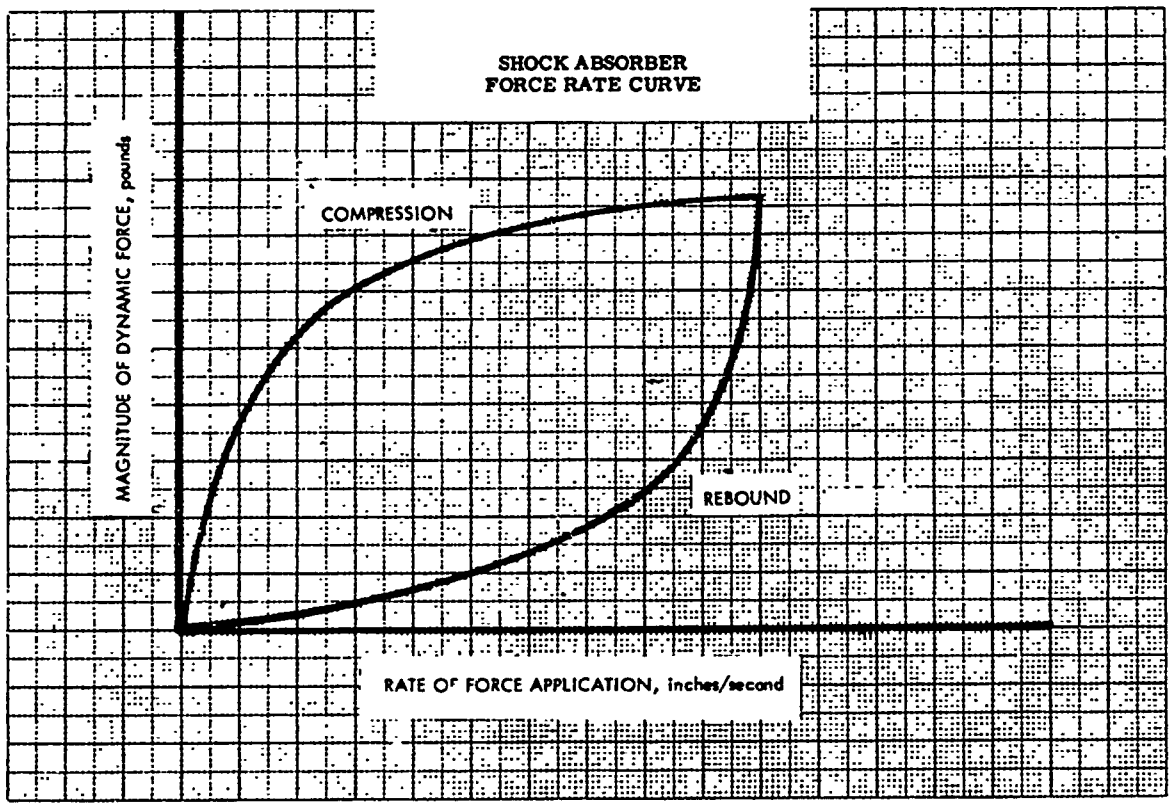
SHOCK ABSORBER
FORCE RATE CURVE
MAGNITUDE OF DYNAMIC FORCE, pounds
COMPRESSION
REBOUND
RATE OF FORCE APPLICATION, inches/second

Fig. 18

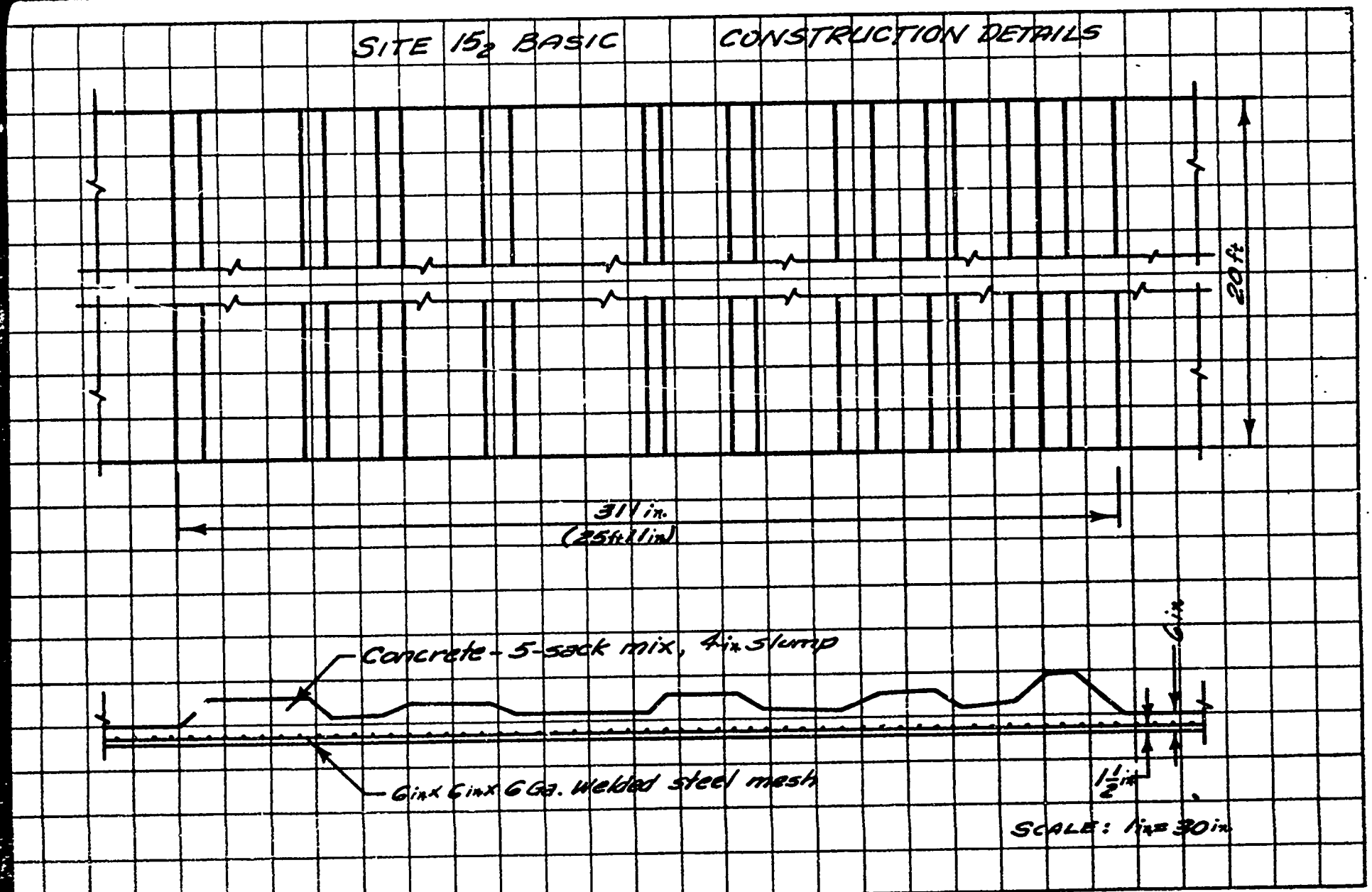

Fig. 19. Sample of course constructed for ride dynamics model

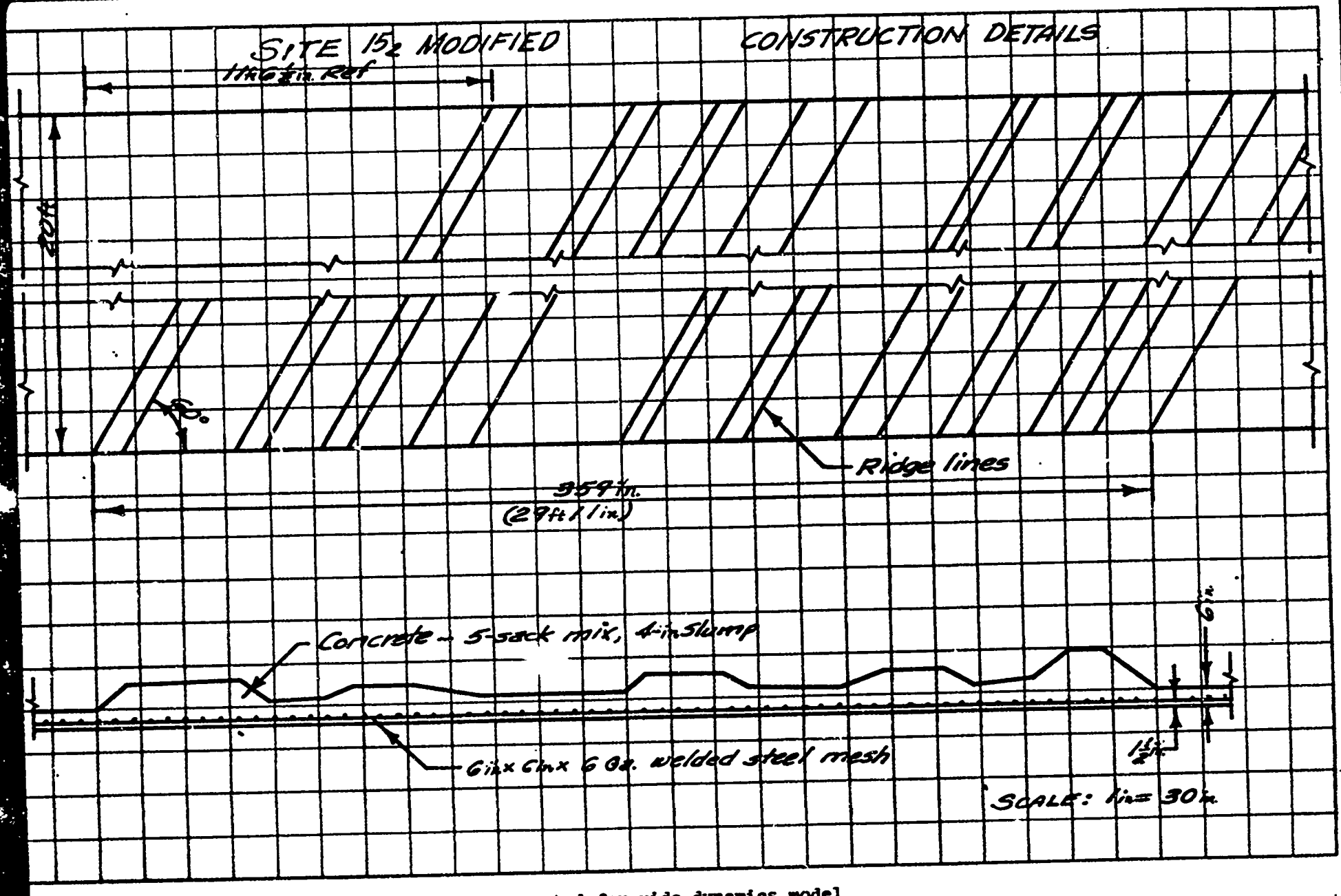

Fig. 20. Sample of course constructed for ride dynamics model

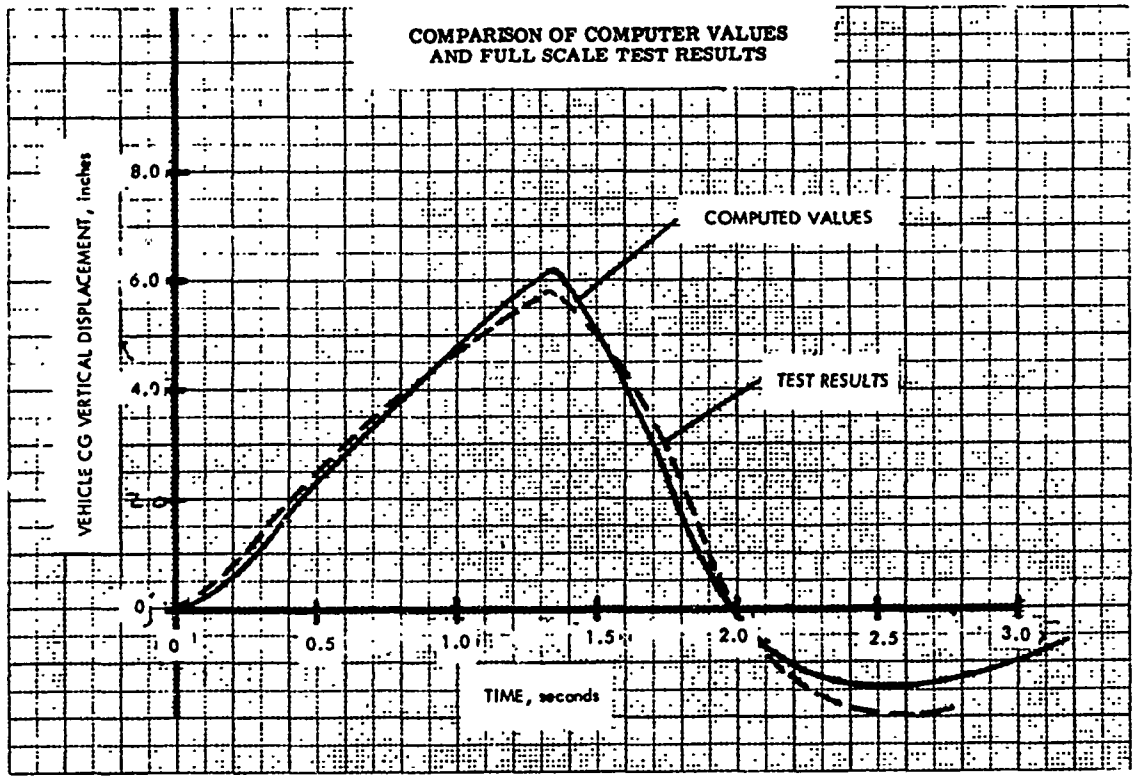
COMPARISON OF COMPUTER VALUES
AND FULL SCALE TEST RESULTS
VEHICLE CG VERTICAL DISPLACEMENT, inches
8.0
6.0
4.0
2.0
0
COMPUTED VALUES
TEST RESULTS
0
0.5
1.0
1.5
2.0
2.5
3.0
TIME, seconds

Fig. 21

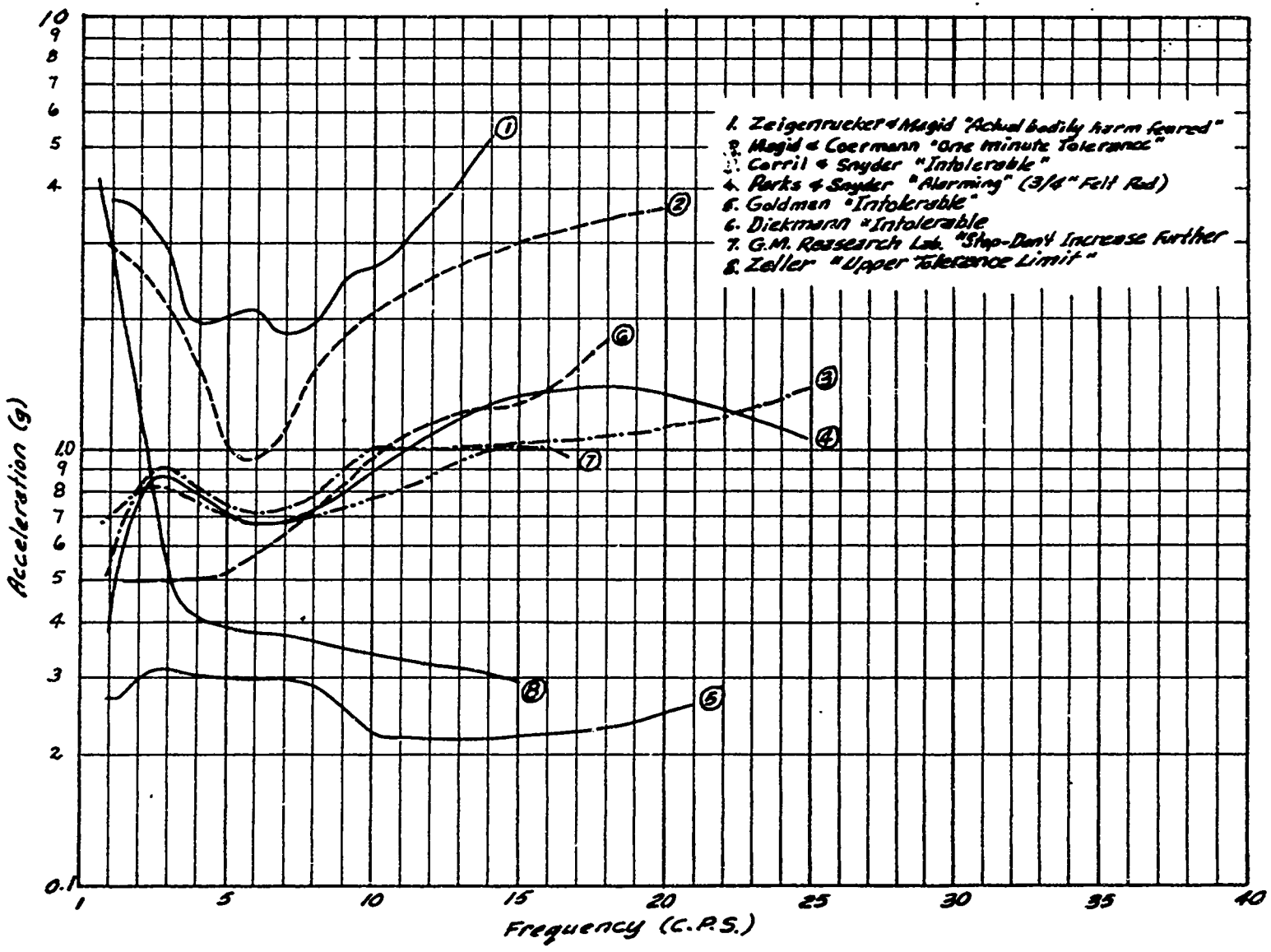

Fig. 22. Vibration tolerance data from various studies

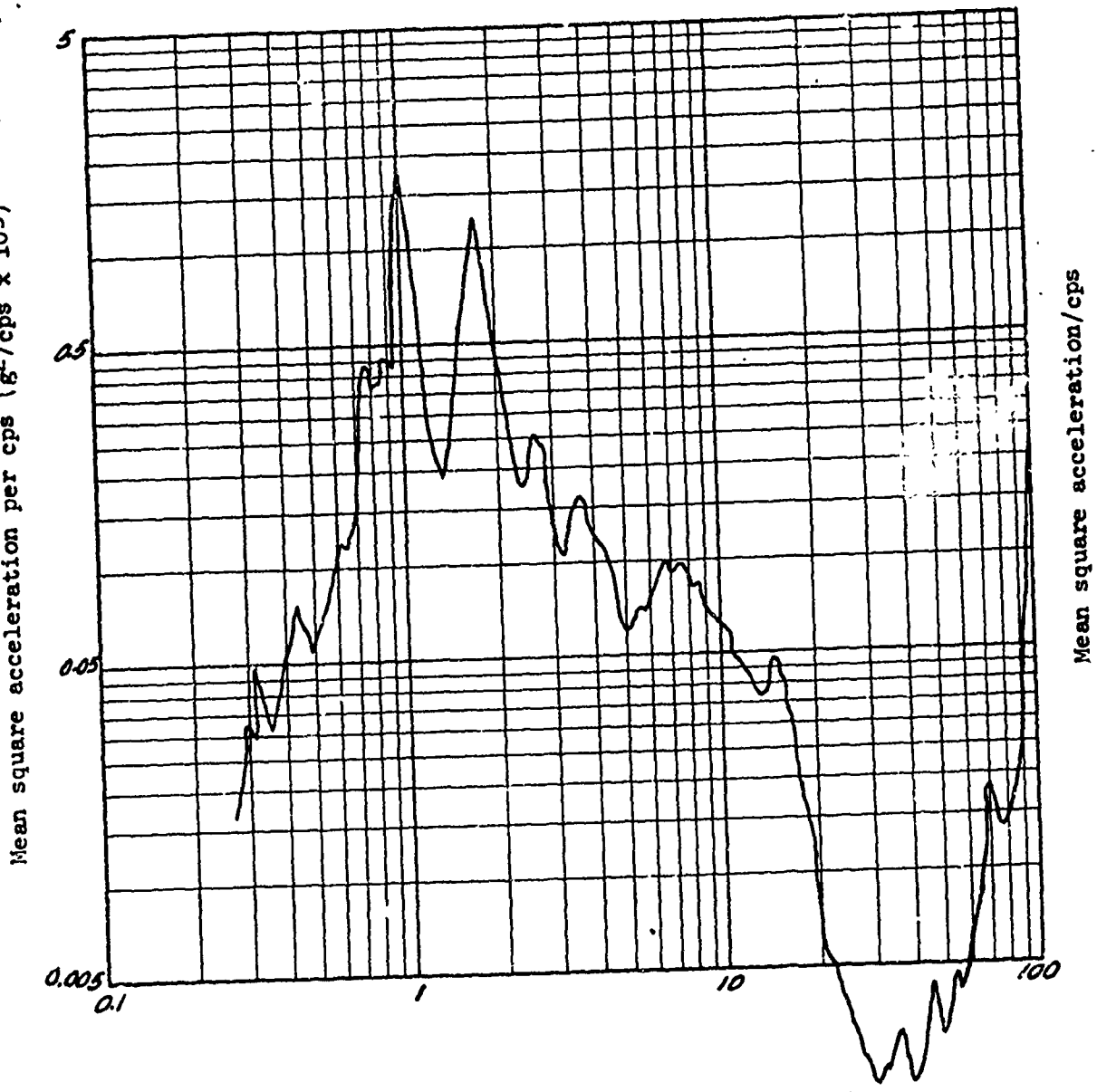

Fig. 23. Measured M37 vertical acceleration power spectral density
(5 mph over 250 ft of cross country terrain)
(Measured at vehicle frame under driver's seat)

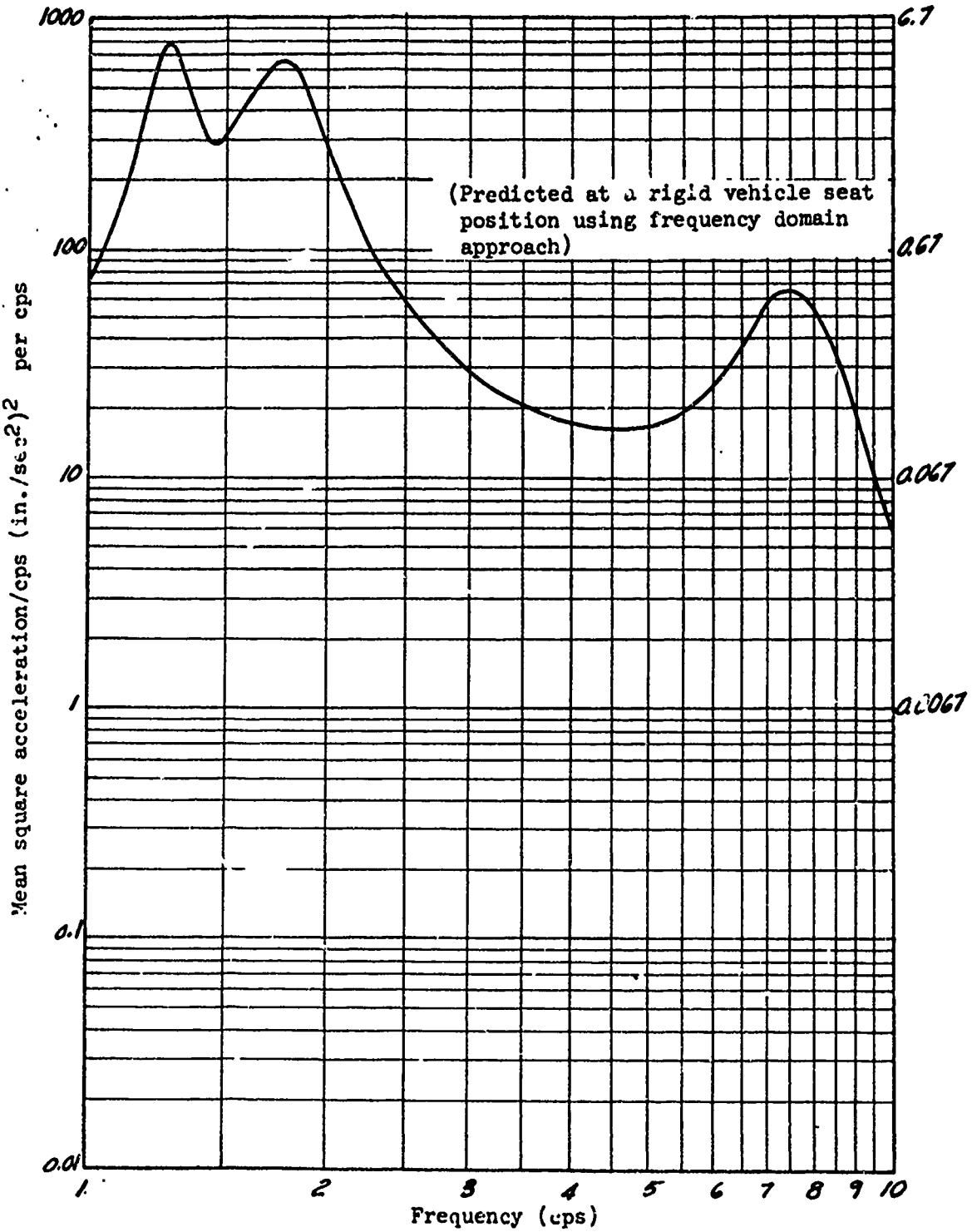

Fig. 24. Output acceleration power spectral density for constant level velocity input power spectral density

P_o (acc) = ω^2 P_o (vel)

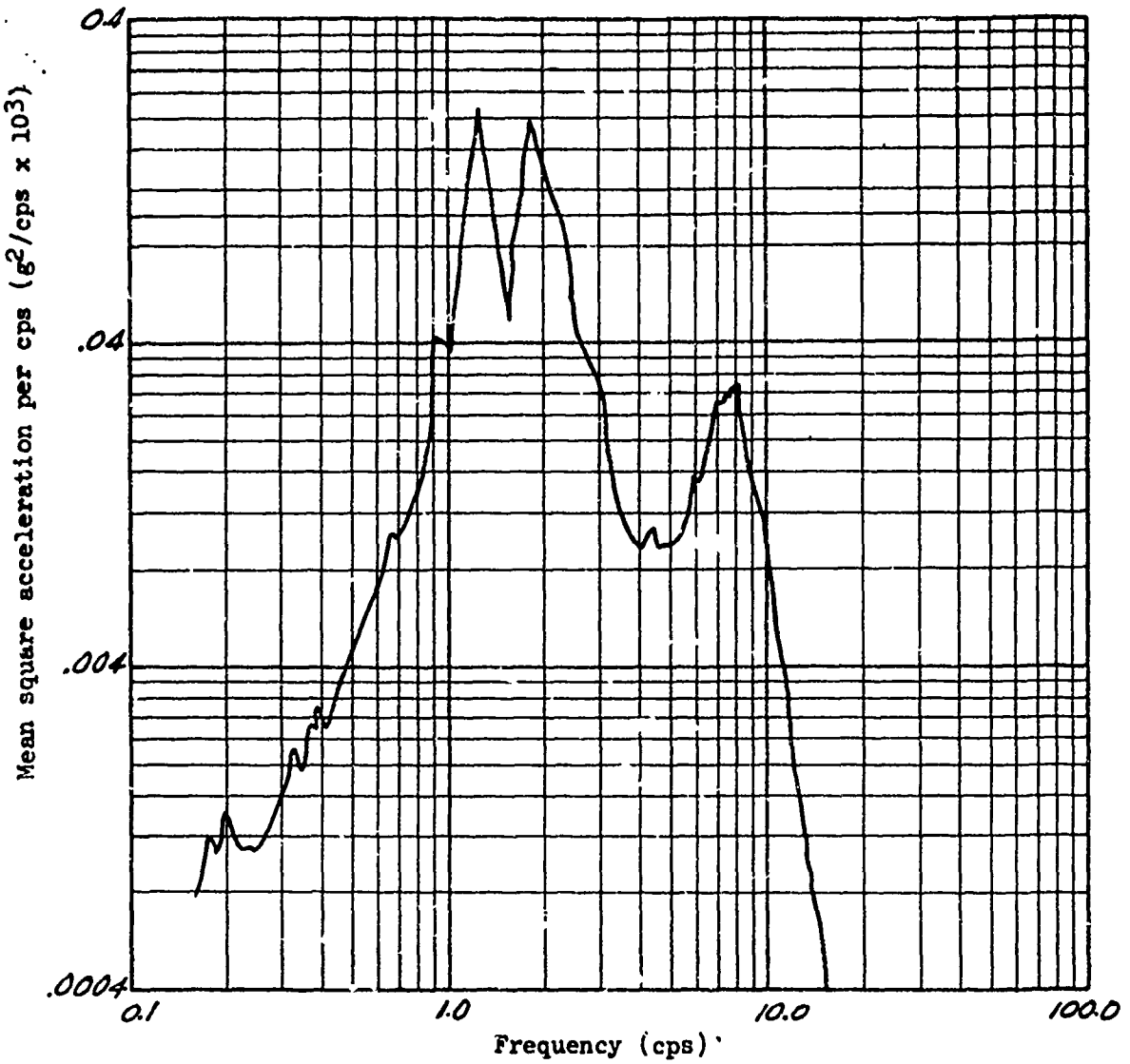

Fig. 25. Power spectral density of vertical seat acceleration with input to left rear wheel only (2 mph). (Recorded terrain input using time domain approach)

ELECTRONIC COMPUTER PROGRAM ABSTRACT

TITLE OF PROGRAM	PROGRAM NO.
Fourier Series Curve Fit for Unequally Spaced Points	04-G1-Z0-007

PREPARING AGENCY

U. S. Army Engineer Waterways Experiment Station, Vicksburg, Miss.

AUTHOR(S)	DATE PROGRAM COMPLETED	STATUS OF PROGRAM	
		PHASE	STATUS
J. F. Smith	March 1965	MOD	OP

A. PURPOSE OF PROGRAM

To compute the amplitude coefficients, c_i, and the phase angles, α_i, for N terms of a Fourier Series to fit a set of M equally or unequally spaced points with linear interpolation between points. The output is used in an equation of the form

$$f(t) = \frac{a_o}{2} + \sum_{i=1}^{N} c_i \sin \left(\frac{2\pi i}{T} t + \alpha_i\right)$$

B. PROGRAM SPECIFICATIONS

The program will accept up to a maximum of 100 coordinate pairs as input and it will compute up to 52 terms in the Fourier Series. A control card contains the number of coordinate pairs, the number of series terms, and flags to obtain output options.

The program is written in FORTRAN-II and uses 1841_{10} words of storage excluding subroutines.

C. METHODS

The Euler formulas are computed using linear interpolation between points to obtain the a_i and b_i coefficients. Then we have

$$c_i = (a_i^2 + b_i^2)$$

and

$$\alpha_i = \tan^{-1} \frac{a_i}{b_i}$$

where i = 1, 2, ..., N.
(See reference for derivation of this equation)

D. EQUIPMENT DETAILS

GE 225 computer, 8K memory, card reader, punch, and on-line printer.

E. INPUT-OUTPUT

Coordinate pairs are punched in 9-column fields, 4 pairs per card; i.e., x_1, y_1, x_2, y_2, x_3, y_3, x_4, y_4, etc. The data with a decimal point can be anywhere in the field. (See write-up for complete input format)

Output is printed listing with optional punch cards of either the normal Euler coefficients and/or the amplitude-phase angle coefficients.

F. ADDITIONAL REMARKS

Original code was written by A. F. Zettlemoyer and C. W. Bowman, Manufacturing Research Space Guidance Center, Oswego, New York.

Reference for the equation derivation is C. R. Wylie, Jr., Advanced Engineering Mathematics, McGraw-Hill, 1951, pp. 113-130.

Write-up, listing, source deck, and binary deck available.

FOURIER SERIES CURVE FIT FOR UNEQUALLY SPACED POINTS

Specifications

Coded by	J. F. Smith, March 1, 1965
Entry	Main Program
Type	FORTRAN-II
Storage	1841_{10} (GE-225)

Purpose

Given a series of coordinates representing a function, to compute the Euler coefficients for a given number of terms of a Fourier Series that best represent the function.

Use

1. The function to be fitted must be expressed in a series of coordinate pairs (up to 100). These pairs may or may not be equally spaced.

2. An input value, N, indicating the number of terms to be computed (up to 52) and a set of flags controlling output options are entered.

3. The output is a listing of the coefficients and the calculated "fit" of the input data. Optional punch card output is also available.

Method

Straight lines are calculated between each set of data points in the slope, c, and intercept, cc, form. Each of these linear equations is used as the f(x) in the interval for the calculation of the Euler coefficients.

The following integrations are performed for a_o, the constant term; a_i, the cosine coefficient; and b_i, the sine coefficient.

$$a_o = \frac{1}{p} \int_o^{2p} f(x)\, dx \qquad (1)$$

$$a_i = \frac{1}{p} \int_o^{2p} f(x) \cos\left(\frac{\pi i}{p} x\right) dx \qquad (2)$$

$$b_i = \frac{1}{p} \int_0^{2p} f(x) \sin \left(\frac{\pi i}{p} x\right) dx \qquad (3)$$

where $2p$ is the fundamental period ($2p = T$), $f(x) = cx + cc$, and $i = 1, 2, \ldots, N$.

To speed up evaluation when using the coefficients to evaluate a forcing function in a dynamic simulation, an alternate form of Fourier Series is used.

$$f(t) = \frac{a_o}{2} + \sum_{i=1}^{N} c_i \sin \left(\frac{2\pi i}{T} t + \alpha_i\right) \qquad (4)$$

where t = independent variable
$f(t)$ = dependent variable
a_o = twice the average value of $f(t)$
c_i = amplitude coefficient for the i^{th} term
α_i = phase angle for the i^{th} term
T = the fundamental period
N = number of terms in the series

To compute c_i and α_i for use in this equation, we have

$$c_i = (a_i^2 + b_i^2)^{\frac{1}{2}} \qquad (5)$$

$$\alpha_i = \tan^{-1} \frac{a_i}{b_i} \qquad (6)$$

where a_i and b_i are from equations (2) and (3) and $i = 1, 2, \ldots, N$.

Data preparation

Card 1	71 Hollerith characters, cols 2-72		
Card 2	Cols 1-10	M	(rt. adjusted in the field)
	11-20	FCN	(anywhere in the field with
	21-30	CARD	a decimal point)
	31-40	ABLIST	
	41-50	ABCARD	
Card 3, 3+n	Cols 1-9	T(1)	(anywhere in the field with
	10-18	AI(1)	a decimal point)
	19-27	T(2)	
	28-36	AI(2)	Continue T(i), AI(i) values,
	37-45	T(3)	4 pairs per card for M pairs.
	46-54	AI(3)	
	55-63	T(4)	
	64-72	AI(4)	

FORTRAN Symbol Definition

M	number of pairs of coordinates
NTH	number of terms in computed series
CARD	1.0 indicates punch ampl. coeff. and angles 0.0 indicates no punch
ABLIST	1.0 indicates print a_i and b_i 0.0 indicates no print
ABCARD	1.0 indicates punch a_i and b_i 0.0 indicates no punch
T(i)	time (or distance) coordinate, i = 1, M
AI(i)	amplitude (or elevation) coordinate, i = 1, M

Output

The 71 Hollerith characters are printed in the heading. The amplitude coefficients and phase angles are printed and an option allows a_i and b_i to be printed.

The tabulation shows the input data, x and f(x), with the calculated f(x) and error with an absolute percent. The full scale error is the maximum absolute error divided by the maximum f(x).

Punch card output is optional. Set CARD = 1.0 and the amplitude coefficients and phase angles are punched out in groups, 4 per card, with E16.7. The output looks as follows:

Card 1	Cols	1-16	a_o	bb±0.FFFFFFFE±xx
		17-32	c(1)	
		33-48	c(2)	
		49-64	c(3)	
Card 2+n	Cols	1-16	c(4)	Continue c(i), 4 per card,
		17-32	c(5)	for N values.
		33-48	c(6)	
		49-64	c(7)	
Card 3	Cols	1-16	T	bb±0.FFFFFFFE±xx
		17-32	$\alpha(1)$	
		33-48	$\alpha(2)$	
		49-64	$\alpha(3)$	
Card 4+n	Cols	1-16	$\alpha(4)$	Continue $\alpha(i)$, 4 per card,
		17-32	$\alpha(5)$	for N values.
		33-48	$\alpha(6)$	
		49-64	$\alpha(7)$	

The optional punch output of a_i and b_i is the same as above; a_o and T are punched and $b_n = 0$. Set ABCARD = 1.0 and output is as follows:

Card 1	Cols 1-16	a_o	bb±0.FFFFFFFE±xx
	17-32	a(1)	
	33-48	a(2)	
	49-64	a(3)	
Card 2+n	Cols 1-16	a(4)	Continue a(i), 4 per card,
	17-32	a(5)	for N values.
	33-48	a(6)	
	49-64	a(7)	
Card 3	Cols 1-16	T	bb±0.FFFFFFFE±xx
	17-32	b(1)	
	33-48	b(2)	
	49-64	b(3)	
Card 4+n	Cols 1-16	b(4)	Continue b(i), 4 per card,
	17-32	b(5)	for N values.
	33-48	b(6)	
	49-64	b(7)	

GE-225 User Notes

1. If function being fitted is to be used in a cyclic manner, then the first and last pairs of data points should agree in amplitude to avoid a discontinuity.

2. The statements to read the coefficients punched by this program into another FORTRAN-II program knowing N are:

```
10      FORMAT (4E16.7)
        READ 10, AO, (C(I), I = 1, N)
        READ 10, T, (ALPHA(I), I = 1, N)
```

OR

```
        READ 10, AO, (A(I), I = 1, N)
        READ 10, T, (B(I), I = 1, N)
```

References

This program was originally written by A. F. Zettlemoyer and C. W. Bowman, Manufacturing Research Space Guidance Center, Oswego, New York.

The derivation of the alternate form of the Fourier Series may be found in C. R. Wylie, Jr., Advanced Engineering Mathematics, McGraw-Hill, 1951, pp. 113-130.

```
C     FOURIER SERIES CURVE FITTING        MARCH 1965          JF SMITH
C
C     UP TO 100 UNEQUALLY SPACED COORDINATE PAIRS ALLOWED AS INPUT
C
C     UP TO 52 TERMS COMPUTED AS OUTPUT
C
C     OUTPUT PRINT OF AMPLITUDE COEFFICIENTS AND PHASE ANGLES
C
C     OPTIONAL CARD OUTPUT OF AMPLITUDE COEFFICIENTS AND PHASE ANGLES
C
C     OPTIONAL PRINT OF THE SINE AND COSINE COEFFICIENTS
C
C     OPTIONAL CARD OUTPUT OF THE SINE AND COSINE COEFFICIENTS
C
C     BY A.F. ZETTLEMOYER AND C.W. BOWMAN, MANUFACTURING RESEARCH
C     SPACE GUIDANCE CENTER, OSWEGO, NEW YORK

      DIMENSION T(100),AI(100),A(52),AA(52),CF(53),AL(53)
      EQUIVALENCE (CF(1),U),(AL(1),PTT)
  105 FORMAT(I10,6E10.8)
  106 FORMAT(8F9.4)
  107 FORMAT(4E16.7)
  120 FORMAT(12X1HX16X4HF(X)11X8HCAL F(X)12X5HERROR10X7HPERCENT)
  121 FORMAT (/// 41X 10HTABULATION   //)
  122 FORMAT(1H ,1P4E18.6,2PF11.2)
  123 FORMAT(1H1,29X,28HFOURIER SERIES CURVE FITTING ///)
  127 FORMAT(72H
     1                )
  128 FORMAT(1H0)
 1002 FORMAT(E20.7,E18.7,41X,I5)
 1005 FORMAT(12X4HA(0)15X1HT)
 1007 FORMAT(/8X12HAMPL. COEFF.6X11HANGLE (RAD)45X1HN)
 1008 FORMAT(1H0,6X,19HFULL SCALE ERROR = ,2PF5.2)
 1009 FORMAT(/8X12HAMPL. COEFF.6X11HANGLE (RAD)10X4HA(N)15X4HB(N)12X1HN)
 1010 FORMAT(E20.7,3E18.7,5X,I5)
C
C     INPUT COMPUTATION LIMITS AND FLAGS
C
   30 READ 127
      READ 105,M,FCN,CARD,ABLIST,ABCARD
      N = M - 1
      NMAX=FCN
C
C     INPUT COORDINATE DATA
C
      READ 106,(T(I),AI(I),I=1,M)
      PTT=T(M)-T(1)
      PT=.5*PTT
      DO 701 I=1,52
      A(I)=0.
  701 AA(I)=0.
      XPI=3.14159265
      FN=1.
      U=0.
C
C     COMPUTE SINE AND COSINE COEFFICIENTS
C
      DO 45 J=1,NMAX
      L=2
      DO 41 I=1,N
```

```
      C=(A(L)-A(I))/(T(L)-T(I))
      CC=A(I)-C*T(I)
      IF(FN-1.0) 22, 22, 23
   22 S=1.0/PT *(C*T(L)*T(L)*0.5+CC*T(L)-C*T(I)*T(I)*0.5)
      V=1.0/PT *(-CC*T(I))
      U=U+S+V
   23 XF=FN*XPI
      XHD=C*PT/(XF*XF)
      XHI=C/XF
      CCX=CC/XF
      XFI=XF*T(I)/PT
      XFL=XF*T(L)/PT
      SXE=SINF(XFL)
      SXG=SINF(XFI)
      DSN=SXE-SXG
      CXE=COSF(XFL)
      CXG=COSF(XFI)
      DCN=CXE-CXG
      A(J)=XHD*DCN+XHI*(T(L)*SXE-T(I)*SXG)+CCX*DSN+A(J)
      AA(J)=XHD*DSN-XHI*(T(L)*CXE-T(I)*CXG)-CCX*DCN+AA(J)
      L=L+1
   41 CONTINUE
      FN=FN+1.
   45 CONTINUE
C
C     PRINT HEADINGS
C
      PRINT 123
      PRINT 127
      PRINT 126
      PRINT 1005
      PRINT 1002,U,PTT
C
C     COMPUTE AMPLITUDE COEFFICIENTS AND PHASE ANGLES
C
      DO 1040 K=1,NMAX
      COAMP = SQRTF(A(K)*A(K) + AA(K)*AA(K))
      AL(K+1)=ATANF(A(K)/AA(K))
 1037 IF(AA(K))1038,1039,1039
 1038 COAMP=-COAMP
 1039 CF(K+1)=COAMP
 1040 CONTINUE
C
C     PRINT OUTPUT
C
      AA(NMAX)=0.0
      IF(ABLIST)1041,1041,1042
 1041 PRINT 1007
      PRINT 1002,(CF(K+1),AL(K+1),K,K=1,NMAX)
      GO TO 1043
 1042 PRINT 1009
      PRINT 1010,(CF(K+1),AL(K+1),A(K),AA(K),K,K=1,NMAX)
 1043 CONTINUE
C
C     PUNCH CARD OUTPUT
C
      IF(CARD)1045,1045,1046
 1046 NCARD=NMAX+1
      PUNCH 107,(CF(K),K=1,NCARD)
      PUNCH 107,(AL(K),K=1,NCARD)
```

```
 1045 CONTINUE
      IF(ARCARD)1047,1047,1048
 1048 PUNCH 107,U,(A(K),K=1,NMAX)
      PUNCH 107,PTT,(AA(K),K=1,NMAX)
 1047 CONTINUE
C
C     COMPUTE AND PRINT FIT AND ERROR OF FIT
C
      X1=.5*U
      XDIFF=0.0
      AMAX=0.0
      DO 1060 I=1,M
      X=X1
      DO 1050 K=1,NMAX
      Z=K
      COAMP=CF(K+1)
      Y=AL(K+1)
 1050 X=X+COAMP*SINF(Z*XPI*T(I)/PT+Y)
      IF(I - 2) 805, 806, 806
  805 PRINT 121
      PRINT 120
  806 DIFF = X - A(I)
      IF(A(I))808,807,808
  807 PCDIF=0.0
      GO TO 809
  808 PCDIF=ABSF(DIFF/A(I))
  809 PRINT 122,T(I),A(I),X,DIFF,PCDIF
      IF(XDIFF-ABSF(DIFF))1030,1031,1031
 1030 XDIFF=ABSF(DIFF)
 1031 IF(AMAX-ABSF(A(I)))1032,1035,1035
 1032 AMAX=ABSF(A(I))
 1035 CONTINUE
 1060 CONTINUE
      XDIFF=XDIFF/AMAX
      PRINT 1006,XDIFF
C
      GO TO 30
      END
```

```
FOURIER FIT TEST DATA  SAMPLE PROBLEM A   8 JUNE 1965   JF SMITH          DATA  1
      71      25.          1.          1.          1.                    DATA  2
.0      -2.0        .01       -2.0        .02       -2.0        .03       -2.0   DATA  3
.04     -2.0        .05       -2.0        .06       -2.0        .07       -2.0   DATA  4
.08     -2.0        .09       -2.0        .10       -2.0        .11       -2.0   DATA  5
.12     -2.0        .13       -2.0        .14       -2.0        .15       -2.0   DATA  6
.16     -2.0        .17       -2.0        .18       -2.0        .19       -2.0   DATA  7
.2      -2.0        .21       -2.0        .22       -1.9        .23       -1.35  DATA  8
.24       .02       .25         .75       .26        1.3        .27        1.9   DATA  9
.28      2.43       .29        3.0        .30       3.11        .31       3.15   DATA 10
.32      3.03       .33       2.90        .34        2.8        .35       2.78   DATA 11
.36      2.78       .37       2.78        .38       2.78        .39       2.78   DATA 12
.40      2.77       .41       2.76        .42       2.73        .43       2.70   DATA 13
.44      2.66       .45       2.60        .46       2.50        .47       2.40   DATA 14
.48      1.20       .49         -.2       .50       -2.0        .51       -2.08  DATA 15
.52     -2.09       .53       -2.05       .54       -2.0        .55       -1.92  DATA 16
.56     -1.9        .57       -1.92       .58       -1.95       .59       -2.0   DATA 17
.60     -2.0        .61       -2.0        .62       -2.0        .63       -2.0   DATA 18
.64     -2.0        .65       -2.0        .66       -2.0        .67       -2.0   DATA 19
.68     -2.0        .69       -2.0        .70       -2.0                         DATA 20
```

FOURIER SERIES CURVE FITTING

RIER FIT TEST DATA SAMPLE PROBLEM A 8 JUNE 1965 JF SMITH

A(0)	T
-0.7642855E+00	0.7000000E+00

AMPL. COEFF.	ANGLE (RAD)	A(N)	B(N)	N
-0.2639392E+01	0.1433546E+01	-0.2614571E+01	-0.3611200E+00	1
0.1266593E+01	0.1301254E+01	0.1220859E+01	0.3372815E+00	2
0.1619213E-01	0.5816975E+00	0.8896656E-02	0.1352903E-01	3
-0.5803331E+00	0.9787432E+00	-0.4815585E+00	-0.3238641E+00	4
0.4223713E+00	0.7278940E+00	0.2810031E+00	0.3153328E+00	5
-0.7426134E-01	-0.1077931E+01	0.6542281E-01	-0.3513690E-01	6
-0.2387062E+00	0.6039692E+00	-0.1355646E+00	-0.1964762E+00	7
0.1519472E+00	-0.1262937E+00	-0.1913901E-01	0.1507371E+00	8
0.1176537E+00	0.1244368E+01	0.1114409E+00	0.3772702E-01	9
-0.1194020E+00	0.4584138E+00	-0.5283850E-01	-0.1070744E+00	10
0.3952108E-01	-0.1063192E+01	-0.3453792E-01	0.1921060E-01	11
0.9360775E-01	0.6097020E+00	0.5360197E-01	0.7674138E-01	12
-0.7324159E-01	0.2066928E+00	-0.1503095E-01	-0.7168264E-01	13
-0.1998052E-01	0.1097311E+01	-0.1778235E-01	-0.9110935E-02	14
0.6323731E-01	0.1551091E+00	0.9769400E-02	0.6247812E-01	15
-0.3589852E-01	-0.2410725E+00	0.8570564E-02	-0.3486042E-01	16
-0.2126490E-01	0.1139477E+00	-0.2417847E-02	-0.2112700E-01	17
0.3773659E-01	-0.3230870E+00	-0.1198119E-01	0.3578409E-01	18
-0.1200203E-01	-0.6723846E+00	0.7475507E-02	-0.9389655E-02	19
-0.1646095E-01	-0.5602277E+00	0.8747006E-02	-0.1394463E-01	20
0.1611557E-01	-0.8321966E+00	-0.1191604E-01	0.1084986E-01	21
0.3594508E-02	-0.7721945E+00	-0.2507921E-02	0.2575038E-02	22
-0.1260595E-01	-0.1173255E+01	0.1162288E-01	-0.4880430E-02	23
0.1167912E-02	-0.9604572E+00	-0.9570500E-03	0.6693835E-03	24
-0.1238799E-01	0.1427233E+01	-0.1226055E-01	0.0000000E+00	25

TABULATION

X	F(X)	CAL F(X)	ERROR	PERCENT
0.0000000E-01	-2.000000E+00	-2.007796E+00	-7.795557E-03	0.39
1.0000000E-02	-2.000000E+00	-1.996401E+00	3.599301E-03	0.18
2.0000000E-02	-2.000000E+00	-1.997043E+00	2.957394E-03	0.15
3.0000000E-02	-2.000000E+00	-2.007522E+00	-7.522304E-03	0.38
4.0000000E-02	-2.000000E+00	-1.992942E+00	7.058417E-03	0.35
5.0000000E-02	-2.000000E+00	-2.001826E+00	-1.825713E-03	0.09
6.0000000E-02	-2.000000E+00	-2.004757E+00	-4.756957E-03	0.24
7.0000000E-02	-2.000000E+00	-1.991695E+00	8.304773E-03	0.42
8.0000000E-02	-2.000000E+00	-2.006324E+00	-6.324332E-03	0.32
9.0000000E-02	-2.000000E+00	-2.000084E+00	-8.354709E-05	0.00
1.0000000E-01	-2.000000E+00	-1.993188E+00	6.812410E-03	0.34
1.1000000E-01	-2.000000E+00	-2.009312E+00	-9.311646E-03	0.47
1.2000000E-01	-2.000000E+00	-1.994437E+00	5.563444E-03	0.28
1.3000000E-01	-2.000000E+00	-1.997574E+00	2.425859E-03	0.12
1.4000000E-01	-2.000000E+00	-2.009632E+00	-9.632260E-03	0.48
1.5000000E-01	-2.000000E+00	-1.988967E+00	1.103261E-02	0.55
1.6000000E-01	-2.000000E+00	-2.004853E+00	-4.853379E-03	0.24
1.7000000E-01	-2.000000E+00	-2.005932E+00	-5.932171E-03	0.30
1.8000000E-01	-2.000000E+00	-1.985115E+00	1.488546E-02	0.74
1.9000000E-01	-2.000000E+00	-2.015529E+00	-1.552910E-02	0.78

[illegible]	-2.000000E+00	-1.995123E+00	4.877325E-03	0.24
2.100000E-01	-2.000000E+00	-1.979338E+00	2.066209E-02	1.03
2.200000E-01	-1.900000E+00	-1.897363E+00	2.637347E-03	0.14
2.300000E-01	-1.350000E+00	-1.224547E+00	1.254531E-01	9.29
2.400000E-01	2.000000E-02	-8.890968E-02	-1.089097E-01	544.55
2.500000E-01	7.500000E-01	7.649811E-01	1.498110E-02	2.00
2.600000E-01	1.300000E+00	1.301688E+00	1.688389E-03	0.13
2.700000E-01	1.900000E+00	1.875147E+00	-2.485264E-02	1.31
2.800000E-01	2.430000E+00	2.467391E+00	3.739059E-02	1.54
2.900000E-01	3.000000E+00	2.924317E+00	-7.568309E-02	2.52
3.000000E-01	3.110000E+00	3.132100E+00	2.210039E-02	0.71
3.100000E-01	3.150000E+00	3.121620E+00	-2.837976E-02	0.90
3.200000E-01	3.030000E+00	3.033195E+00	3.194928E-03	0.11
3.300000E-01	2.900000E+00	2.905005E+00	5.005337E-03	0.17
3.400000E-01	2.800000E+00	2.802990E+00	2.989691E-03	0.11
3.500000E-01	2.780000E+00	2.784385E+00	4.384723E-03	0.16
3.600000E-01	2.780000E+00	2.779448E+00	-5.520657E-04	0.02
3.700000E-01	2.780000E+00	2.777886E+00	-2.114005E-03	0.08
3.800000E-01	2.780000E+00	2.784196E+00	4.195947E-03	0.15
3.900000E-01	2.780000E+00	2.774129E+00	-5.870745E-03	0.21
4.000000E-01	2.770000E+00	2.773851E+00	3.850516E-03	0.14
4.100000E-01	2.760000E+00	2.758091E+00	-1.909409E-03	0.07
4.200000E-01	2.730000E+00	2.725149E+00	-4.850894E-03	0.18
4.300000E-01	2.700000E+00	2.707503E+00	7.502850E-03	0.28
4.400000E-01	2.660000E+00	2.652956E+00	-7.044449E-03	0.26
4.500000E-01	2.600000E+00	2.588263E+00	-1.173666E-02	0.45
4.600000E-01	2.500000E+00	2.537562E+00	3.756167E-02	1.50
4.700000E-01	2.400000E+00	2.238146E+00	-1.618540E-01	6.74
4.800000E-01	1.200000E+00	1.274798E+00	7.479822E-02	6.23
4.900000E-01	-2.000000E-01	-3.446057E-01	-1.446057E-01	72.30
5.000000E-01	-2.000000E+00	-1.743440E+00	2.565604E-01	12.83
5.100000E-01	-2.080000E+00	-2.152685E+00	-7.268480E-02	3.49
5.200000E-01	-2.090000E+00	-2.049929E+00	4.007091E-02	1.92
5.300000E-01	-2.050000E+00	-2.054098E+00	-4.097831E-03	0.20
5.400000E-01	-2.000000E+00	-2.010779E+00	-1.077857E-02	0.54
5.500000E-01	-1.920000E+00	-1.907840E+00	1.216040E-02	0.63
5.600000E-01	-1.900000E+00	-1.913723E+00	-1.372324E-02	0.72
5.700000E-01	-1.920000E+00	-1.921479E+00	-1.479117E-03	0.08
5.800000E-01	-1.950000E+00	-1.943676E+00	6.324343E-03	0.32
5.900000E-01	-2.000000E+00	-2.003613E+00	-3.612798E-03	0.18
6.000000E-01	-2.000000E+00	-1.998245E+00	1.754805E-03	0.09
6.100000E-01	-2.000000E+00	-1.994207E+00	5.793437E-03	0.29
6.200000E-01	-2.000000E+00	-2.009777E+00	-9.777188E-03	0.49
6.300000E-01	-2.000000E+00	-1.992477E+00	7.523259E-03	0.38
6.400000E-01	-2.000000E+00	-2.000719E+00	-7.189810E-04	0.04
6.500000E-01	-2.000000E+00	-2.006106E+00	-6.107893E-03	0.31
6.600000E-01	-2.000000E+00	-1.991373E+00	8.627173E-03	0.43
6.700000E-01	-2.000000E+00	-2.005434E+00	-5.433645E-03	0.27
6.800000E-01	-2.000000E+00	-2.001178E+00	-1.177821E-03	0.06
6.900000E-01	-2.000000E+00	-1.993198E+00	6.802071E-03	0.34
7.000000E-01	-2.000000E+00	-2.007796E+00	-7.795572E-03	0.39

FULL SCALE ERROR = 8.14

(Listing of punched card output)

```
-0.7642855E+00  -0.2639392E+01   0.1266593E+01   0.1619213E-01
-0.5803331E+00   0.4223713E+00  -0.7426134E-01  -0.2387062E+00
 0.1519472E+00   0.1176537E+00  -0.1194020E+00   0.3952108E-01
 0.9360775E-01  -0.7324159E-01  -0.1998052E-01   0.6323731E-01
-0.3589852E-01  -0.2126490E-01   0.3773659E-01  -0.1200203E-01
-0.1046095E-01   0.1611557E-01   0.3594508E-02  -0.1260595E-01
 0.1167912E-02  -0.1238799E-01
 0.7000000E+00   0.1433546E+01   0.1301254E+01   0.5816975E+00
 0.9787432E+00   0.7278940E+00  -0.1077931E+01   0.6039692E+00
-0.1262937E+00   0.1244368E+01   0.4584138E+00  -0.1063192E+01
 0.6097020E+00   0.2066928E+00   0.1097311E+01   0.1551091E+00
-0.2410725E+00   0.1139477E+00  -0.3230870E+00  -0.6723846E+00
-0.5602277E+00  -0.8321966E+00  -0.7721945E+00  -0.1173255E+01
-0.9604572E+00   0.1427233E+01
-0.7642855E+00  -0.2614571E+01   0.1220859E+01   0.8896656E-02
-0.4815565E+00   0.2810031E+00   0.6542281E-01  -0.1355646E+00
-0.1913901E-01   0.1114409E+00  -0.5283850E-01  -0.3453792E-01
 0.5360197E-01  -0.1503095E-01  -0.1778235E-01   0.9769400E-02
 0.8570564E-02  -0.2417847E-02  -0.1198119E-01   0.7475507E-02
 0.8747006E-02  -0.1191604E-01  -0.2507991E-02   0.1162288E-01
-0.9570500E-03  -0.1226055E-01
 0.7000000E+00  -0.3611200E+00   0.3372815E+00   0.1352903E-01
-0.3238641E+00   0.3153328E+00  -0.3513690E-01  -0.1964762E+00
 0.1507371E+00   0.3772702E-01  -0.1070744E+00   0.1921060E-01
 0.7674138E-01  -0.7168264E-01  -0.9110935E-02   0.6247812E-01
-0.3486042E-01  -0.2112700E-01   0.3578409E-01  -0.9389655E-02
-0.1394463E-01   0.1084986E-01   0.2575038E-02  -0.4880430E-02
 0.6693835E-03   0.0000000E+00
```

TEST SITE 15/2 REVERSED WITH EXTENDED FLAT. 19 MARCH 1965

21 20.0 DATA 1

0.0	0.0	9.0	9.0	42.0	10.0	50.0	2.0	DATA 2
67.0	3.0	75.0	7.0	102.0	7.0	111.0	3.0	DATA 3
155.0	3.0	161.0	9.0	184.0	9.0	192.0	4.0	DATA 4
219.0	3.0	231.0	8.0	249.0	9.0	258.0	3.0	DATA 5
270.0	5.0	286.0	14.0	295.0	15.0	311.0	0.0	DATA 6
600.0	0.0							DATA 7

FOURIER SERIES CURVE FITTING

TEST SITE 15/2 REVERSED WITH EXTENDED FLAT. 19 MARCH 1965

A(0)	T
.6435000E+01	0.6000000E+03

AMPL. COFFF.	ANGLE (RAD)	N
.3562693E+01	-0.1385969E+00	1
.1097255E+01	-0.1447923E+01	2
.1697494E+01	-0.1122497E+00	3
.7943564E+00	0.1146640E+01	4
.1368509E+01	-0.5424566E+00	5
.6257984E+00	-0.1145065E+01	6
.1009733E+01	0.8843362E-01	7
.1047018E+01	0.2741805E+00	8
.1733835E+01	-0.1124541E+01	9
.6235158E+00	-0.6464449E+00	10
.1283778E+01	-0.7717952E+00	11
.8276767E+00	0.1377178E+00	12
.4114004E+00	-0.4727633E+00	13
.5376203E+00	-0.4299839E+00	14
.5963749E+00	0.1830770E-01	15
.2398567E+00	0.4026079E+00	16
.2841937E+00	0.2416877E+00	17
.1258216E+00	0.9278563E+00	18
.4714055E+00	-0.3523176E+00	19
.1629668E+00	-0.1318209E+01	20

TABULATION

X	F(X)	CAL F(X)	ERROR	PERCENT
.0000000E-01	0.0000000E-01	2.188267E+00	2.188267E+00	0.00
.6000000E+00	9.000000E+00	7.058781E+00	-1.941219E+00	21.57
.2000000E+01	1.000000E+01	8.059029E+00	-1.940971E+00	19.41
.3000000E+01	2.000000E+00	4.194965E+00	2.194965E+00	109.75
.3700000E+01	3.000000E+00	3.568864E+00	5.688640E-01	18.96
.5000000E+01	7.000000E+00	6.403217E+00	-5.967827E-01	8.53
.6200000E+02	7.000000E+00	6.197643E+00	-8.023574E-01	11.46
.1100000E+02	3.000000E+00	4.091230E+00	1.091230E+00	36.37
.1550000E+02	3.000000E+00	4.365994E+00	1.365994E+00	45.53
.1610000E+02	9.000000E+00	7.125314E+00	-1.874686E+00	20.83
.1840000E+02	9.000000E+00	7.272785E+00	-1.727215E+00	19.19
.2300000E+02	4.000000E+00	5.291227E+00	1.291227E+00	32.28
.2490000E+02	3.000000E+00	3.849692E+00	8.496923E-01	28.32
.2310000E+02	8.000000E+00	7.436570E+00	-5.634298E-01	7.04
.2490000E+02	9.000000E+00	7.787056E+00	-1.212944E+00	13.48
.2580000E+02	3.000000E+00	4.765935E+00	1.765935E+00	58.86
.2760000E+02	5.000000E+00	6.253651E+00	1.253651E+00	25.07
.2860000E+02	1.400000E+01	1.345447E+01	-5.455294E-01	3.90
.2950000E+02	1.500000E+01	1.368741E+01	-1.312590E+00	8.75
.3110000E+02	3.000000E-01	1.365068E+00	1.365068E+00	0.00
.3600000E+02	0.000000E-01	2.188267E+00	2.188267E+00	0.00

FULL SCALE ERROR = 14.63